THE ASTROPHYSICAL JOURNAL, 258:467–489, 1982 July 15

EXTRAGALACTIC CO: GAS DISTRIBUTIONS WHICH FOLLOW THE LIGHT IN IC 342 AND NGC 6946

JUDITH S. YOUNG[1] AND NICK SCOVILLE[1,2]
Received 1981 June 9; accepted 1982 February 8

ABSTRACT

The CO emission in the two Scd galaxies, IC 342 and NGC 6946, has been mapped using the 14 m FCRAO telescope (HPBW = 50″). *In each galaxy, the radial distribution of* CO *out to* $R \approx 10$ *kpc exhibits a falloff which follows the exponential luminosity profile from the stellar disk.* Neither galaxy shows a breach in the molecular gas like that found in our Galaxy between the nucleus and the molecular cloud annulus. The occurrence of this gap in our own Galaxy, but in neither of the external galaxies, suggests a possible link between the deficiency of gas and the presence of either a nuclear bulge or inner Lindblad resonance (ILR). From its rotation curve, the Milky Way has a large nuclear bulge and also has an ILR expected in the vicinity of the hole in the CO distribution. The CO rotation curves for IC 342 and NGC 6946 agree well with previous H I observations; at the present resolution these galaxies appear to undergo nearly rigid rotation inside $R = 5$ kpc and therefore have no ILRs and have small nuclear bulges. Further support for the association of the gap with the ILR or bulge is provided by brief observations reported here of NGC 4321, a more distant Sc galaxy with a rotation curve similar to the Milky Way; the CO distribution appears like that in our own Galaxy with coarser resolution.

A global spiral structure is not evident from the molecular data. We do find several positions with strong CO emission on the optical arms, but not all arms are associated with strong CO emission. The derived H_2 masses in IC 342 and NGC 6946 are, respectively, $\sim 4 \times 10^9\ M_\odot$ at $R < 8$ kpc and $\sim 1 \times 10^{10}\ M_\odot$ at $R < 12$ kpc. In both galaxies the total mass of H_2 inside $R \approx 10$ kpc exceeds that in H I by about a factor of three. In the nuclei the ratio of $H_2/H\ I \approx 50$.

Subject headings: galaxies: individual — galaxies: internal motions — galaxies: structure — interstellar: abundances — interstellar: molecules

I. INTRODUCTION

In spiral galaxies, the distribution and abundance of dense interstellar matter are critical in determining both the morphology and evolution of the disk. It is within the giant molecular clouds that interstellar gas is cycled into the next generation of stars; it is the most massive of these young stars which produce a major part of the galactic luminosity. Surveys of CO emission from the Milky Way indicate that this gas shows strong maxima within 400 pc of the galactic center and in a ring at radii 4 to 8 kpc (Scoville and Solomon 1975; Burton *et al.* 1975). Neither the origin nor the extent to which this distribution is typical of other late type spiral galaxies is presently known.

CO was first detected in external galaxies by Rickard *et al.* (1975) and has since been reported in a total of about a dozen galaxies (Rickard *et al.* 1977; Rickard, Turner, and Palmer 1977; Huggins *et al.* 1975; Solomon and de Zafra 1975; Combes *et al.* 1977, 1978; Morris and Lo 1978; Encrenaz *et al.* 1979; Rowan-Robinson, Phillips, and White 1980; Elmegreen, Elmegreen, and Morris 1980; Bieging *et al.* 1981; Blitz *et al.* 1981; Rickard and Palmer 1981). Though several galaxies have been at least partially mapped in CO, the angular resolution and sensitivity have usually biased past studies toward either the central regions of the most active, perhaps atypical, galaxies (e.g., M82 and NGC 253) or isolated concentrations of H II regions or dust in the outer disks of more normal spirals (e.g., M31 and M101). As was found in our own Galaxy, 11 out of 14 external galaxies (excepting M31, M81, and LMC) show the strongest CO emission from the nucleus (Rickard 1979; Rickard *et al.* 1975, 1977; Rickard, Turner, and Palmer 1977; Combes *et al.* 1977; Morris and Lo 1978; Scoville and Young 1982; Young, Scoville, and Tacconi 1982).

Here we report observations of CO in two Scd galaxies, IC 342 and NGC 6946. The data are of sufficient sensitivity and completeness to yield accurate radial distributions for comparison with that in our own Galaxy. Both galaxies are nearly face-on and large in

[1]Five College Radio Astronomy Observatory, University of Massachusetts.
[2]Institute for Astronomy, University of Hawaii.

optical angular diameter ($>10'$); they thus present an ideal opportunity to study the molecular content in detail and to compare with optical and H I data. The angular resolution employed on these two galaxies (50″) allows clear separation of the nuclear and disk components as well as comparison of spiral arm and interarm regions.

Both IC 342 and NGC 6946 are located outside of the Local Group. Ables (1971) has made a photometric study of these galaxies and derived their B luminosity profiles. In both galaxies the H I distributions, mapped by aperture synthesis at $\gtrsim 2'$ resolution (Rogstad and Shostak 1972; Rogstad, Shostak, and Rots 1973; Newton 1980*b*), exhibit central depressions within $R \approx 8$ kpc. The radio continuum emission has been mapped in both galaxies (van der Kruit 1973; van der Kruit, Allen and Rots 1977). Their nuclei show strong infrared emission (Becklin *et al.* 1980; Telesco and Harper 1980; Rieke and Lebofsky 1978); the CO emission was originally detected and partially mapped by Morris and Lo (1978) and has since been mapped concurrently by us and by Rickard and Palmer (1981). Six supernovae have been observed in NGC 6946 in the past 100 years, at least one of which was associated with the prominent arm which led Arp to place this galaxy in the *Atlas of Peculiar Galaxies* (Arp 1966).

The distances to IC 342 and NGC 6946 are uncertain since both galaxies are at low galactic latitudes and suffer large amounts of extinction. De Vaucouleurs (1979) finds distances of 3 and 5 Mpc for IC 342 and NGC 6946 respectively. For IC 342, Sandage and Tammann (1974) gave a distance of 8 Mpc; but this was apparently revised downward to 4 ± 1 Mpc (Tammann as communicated by Baker *et al.* 1977). In the case of NGC 6946, they give a distance of 10 Mpc which is twice that given by de Vaucouleurs. Henceforth, we will adopt distances of 4.5 and 10 Mpc for IC 342 and NGC 6946—partly to be consistent with previous studies of these galaxies (Rogstad and Shostak 1972; van der Kruit, Allen, and Rots 1977; Morris and Lo 1978; Newton 1980*a*). Using the luminosities given by Rogstad and Shostak (1972), the absolute (blue) magnitudes for IC 342 and NGC 6946 are -21 and -22, respectively.

II. OBSERVATIONS

The observations reported here were made between 1980 November and 1981 March with the 14 m antenna of the Five College Radio Astronomy Observatory (FCRAO).[3] At the CO $J = 1 \rightarrow 0$ frequency (115.2712 GHz), the half-power beam width (HPBW) of the telescope is 50″. At a resolution of 50″, one beam width corresponds to 1.1 kpc on IC 342 and 2.4 kpc on NGC 6946. Pointing was checked periodically on Jupiter and was found to be accurate to 4″ rms. The observations were made with a cooled mixer receiver with a single sideband temperature of 500 K. Spectral resolution was provided by a 256 channel filter-bank with 1 MHz channels (2.6 km s^{-1} per MHz at CO). The data were obtained by position switching every 30 s by 10′ and 20′, respectively, for NGC 6946 and IC 342 for an average of 2 hr of integration per point and a total of 150 hours on both galaxies. Because of the low radial velocities of these galaxies, 25 and 40 km s^{-1} for IC 342 and NGC 6946, respectively, there is a possibility of contamination with galactic CO emission (Morris and Lo 1978). In our observations the same off position was used for all points in each galaxy. There is no evidence for Milky Way emission near 0 km s^{-1} or contamination in the off positions (which would appear as dips near 0 km s^{-1}).

Intensity calibration was performed in two steps. First, during the course of an observing run, the receiver sensitivity and atmospheric absorption were monitored and compensated for by observation of an ambient temperature chopper wheel (Penzias and Burrus 1973). A second calibration is needed to correct for antenna and radome losses in order that our data may be compared with those obtained on other telescopes. Since ultimately we wish to compare the CO emissivities in IC 342 and NGC 6946 with those deduced from surveys of our own galactic disk made on the 11 m NRAO antenna (Burton and Gordon 1978; Solomon, Scoville, and Sanders 1982), we scale our intensities to sources measured at NRAO. To accomplish this, we have observed at both FCRAO and NRAO a set of four objects (Table 1), ranging from an extended, "uniform" dark cloud (L134) to the star CIT 6 which is essentially a point source for both antennas. After the raw data from FCRAO are corrected by a factor of 1.68 the measured T_A^* at FCRAO for L134 agrees within the statistical 1 σ uncertainty with that obtained at NRAO, but for CIT 6 is a factor of 1.6 higher at FCRAO as is expected from the ratio of beamwidths of the two telescopes.

As an independent check of the calibration of our observations relative to the NRAO 11 m antenna, we compare our extragalactic CO intensities with recent observations of IC 342 and NGC 6946 by Rickard and Palmer (1981) on the 11 m antenna. At common positions observed in the disks of these galaxies, our intensities agree to within $\pm 10\%$ of those observed on the 11 m. In the nuclei our intensities are a factor of 1.4 times higher, suggesting that the nuclear emission is confined to a region smaller than both beams, $\sim 30''$ across.[4]

[3]The FCRAO is operated with support from the National Science Foundation under grant AST80 26702 and with the permission of the Metropolitan District Commission, Commonwealth of Massachusetts.

[4]Morris and Lo 1978 have measured intensities in the nuclei of IC 342 and NGC 6946 which are a factor of 1.2 to 1.3 lower than those measured by Rickard and Palmer 1981 *on the same telescope*. We do not understand the origin of this discrepancy, nor do

TABLE 1

CO CALIBRATION SOURCES AT FCRAO AND NRAO

SOURCE	α (1950)	δ (1950)	V_{LSR} (km s^{-1})	T_A^*(K) FCRAO[a]	T_A^*(K) NRAO	FCRAO/NRAO
L134	$15^h50^m50^s0$	−04°35′00″	2.7	8.7	8.7	1.00
Orion KL	5 32 46.8	−05 24 28	8.9	62	60	1.03
IRC +10216 ...	9 45 14.0	+13 30 40	−26.0	5.2	4.7	1.11
CIT 6	10 13 12.0	+30 49 24	−1.5	1.25	0.77	1.60

[a]The factor of 1.68 applied to the raw FCRAO intensities corrects for spillover which is included in the NRAO calibration. The beam efficiency measured at FCRAO (0.37) when applied to raw FCRAO intensities yields a value of 95 K for Orion KL.

The positions where our observations were made in the external galaxies are shown superposed on photographs of IC 342 and NGC 6946 in Figure 1. The 33 observations in IC 342, spaced by 45″ or 1 kpc, extend 9 kpc from the nucleus in the north and south directions and 8 kpc in the east and west directions. Two points in IC 342 (one on the nucleus and one in the outer disk at $R \sim 6$ kpc) were also observed in the less saturated ^{13}CO line. In NGC 6946, where the 45″ spacing corresponds to 2.2 kpc, 23 positions were observed within 13 kpc of the nucleus.

The spectra obtained along the north-south axis of IC 342 and the northeast-southwest axis of NGC 6946, indicated in Figure 1, are shown in Figures 2*a* and 2*b*. Table 2 lists: (1) the observed positions as offsets from the nucleus ($\Delta\alpha, \Delta\delta$), (2) peak antenna temperatures (T_A^*), (3) integrated areas ($I = \int T_A^* dV$), (4) peak velocities, and (5) mean velocities. Also included in Table 2 are the line widths, ΔV, defined as the area (I) divided by the peak antenna temperature.[5] For a few positions in the outer regions of the galaxies no CO emission was detected, and for these Table 2 gives 2 σ upper limits.[6]

III. RESULTS

In both galaxies the CO spectra exhibit velocity and intensity changes which correlate well with galactic location. The highest intensities (peak and integrated) are observed in the nuclei with systematic, fairly smooth falloffs at larger galactic radii. The mean velocities vary regularly across both galaxies in the sense expected from galactic rotation. The observed linewidths are largest in the nuclei ($\Delta V_{FWHM} = 71$ and 133 km s^{-1} for IC 342 and NGC 6946, respectively), decreasing by a factor of 2–3 in the disks at $R > 4$ kpc.

The line shapes observed in the nuclei where the rotation curve is steep are sensitive to the resolution of the telescope. With higher resolution observations, a smaller portion of the rotation curve is included in each beam, resulting in narrower spectral lines. The large line-width observed in the nucleus of NGC 6946 is due to the higher inclination of the galaxy and the lower spatial resolution.

a) *The* CO *Radial Distributions*

The dependence of the CO emission on radius in IC 342 and NGC 6946, obtained from line integrals averaged over positions symmetric about the galactic centers, is presented in Figures 3*a* and 3*b*. In both galaxies we measure a smooth intensity decrease with radius which is markedly different from the central peak and ring seen in the Milky Way (Scoville and Solomon 1975). To facilitate the comparison with the Milky Way, we also show in Figures 3*a* and 3*b* the integrated intensities expected for our own Galaxy, derived from the CO emissivity measured as a function of R and Z in the Milky Way (Solomon, Sanders, and Scoville 1978; Burton and Gordon 1978; Bania 1980; Sanders, Solomon, and Scoville 1981), and viewed at the same resolution, inclination, and position angles as the two

Rickard and Palmer 1981 discuss it in their paper. The measurements of Encrenaz *et al.* 1979 made on IC 342 at Bell Labs with a 7 m antenna are low by factors of 2.5 and 3.4 relative to the intensities measured at NRAO (Rickard and Palmer 1981) and FCRAO, respectively. These observations require that the nuclear emission be extended over a region only $\sim 1'$ across.

[5]Since the peak antenna temperatures were measured on spectra smoothed to a resolution of 10 km s^{-1} which is much less than any measured widths, this definition yields a line width measure less susceptible to noise fluctuation than the actual full width at half-intensity measured on unsmoothed data. For a triangular or rectangular profile, ΔV defined above will be the same as the full width at half-intensity.

[6]Since these limits were *measured* from the individual spectra at the time a linear baseline was fit to the end points, the error estimates *include* uncertainties due to baseline curvature. At two positions in NGC 6946 (3′ NE and 45″ SW) a few of the individual spectra showed evidence of standing waves (roughly sinusoidal baseline ripple extending over the *entire* bandpass). These observations, all of which were taken in marginal weather, were omitted from the averages. Inasmuch as the analysis here is based on line fluxes integrated over a velocity interval corresponding to several cycles of the expected telescope standing wave, any small residual standing waves contribute minimal uncertainty.

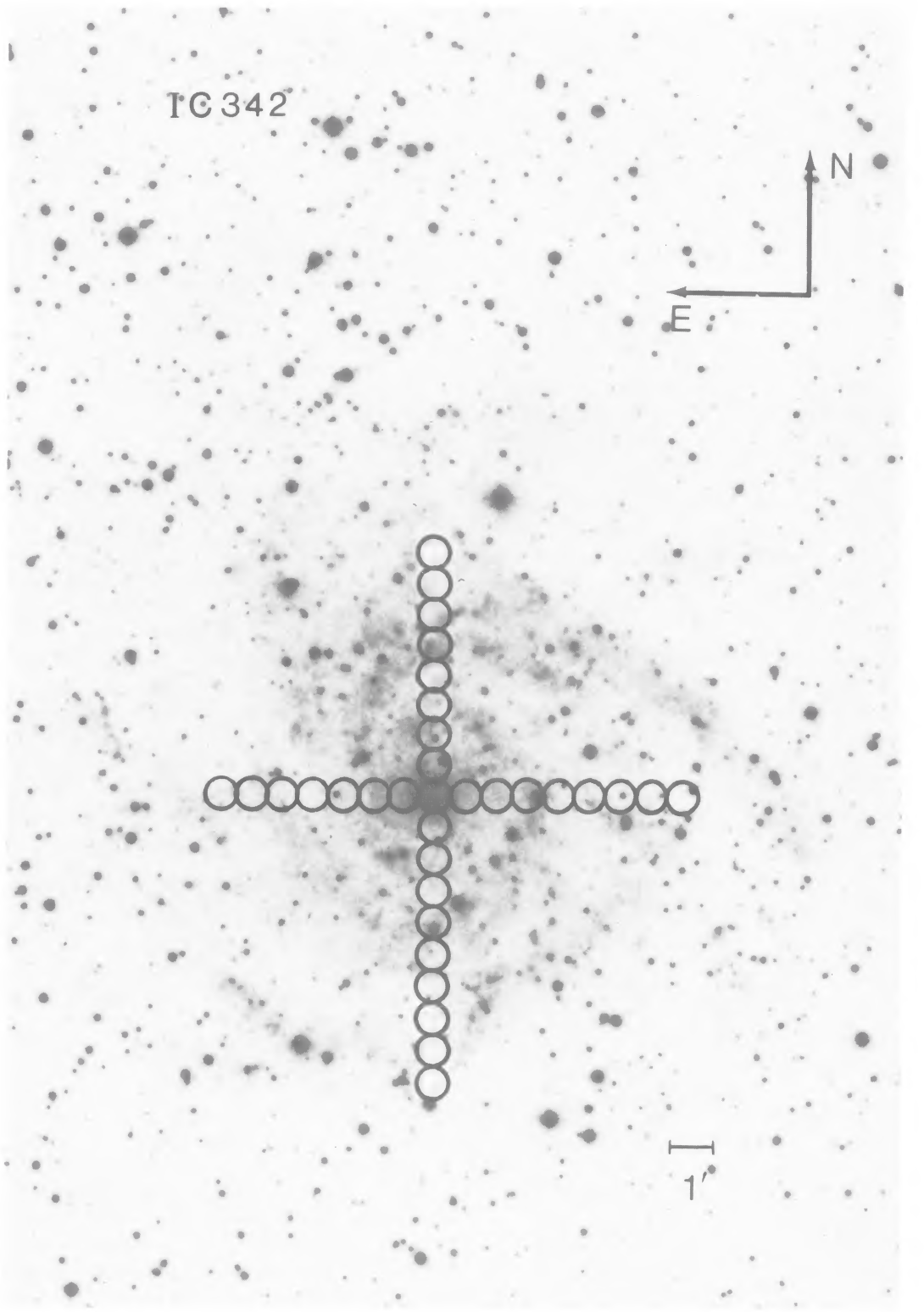

FIG. 1*a*

FIG. 1*a*.—Enlargement from blue Palomar Sky Survey plate of IC 342. Circles are 50″ in diameter (1.1 kpc) and represent positions where observations were made, spaced by 45″.

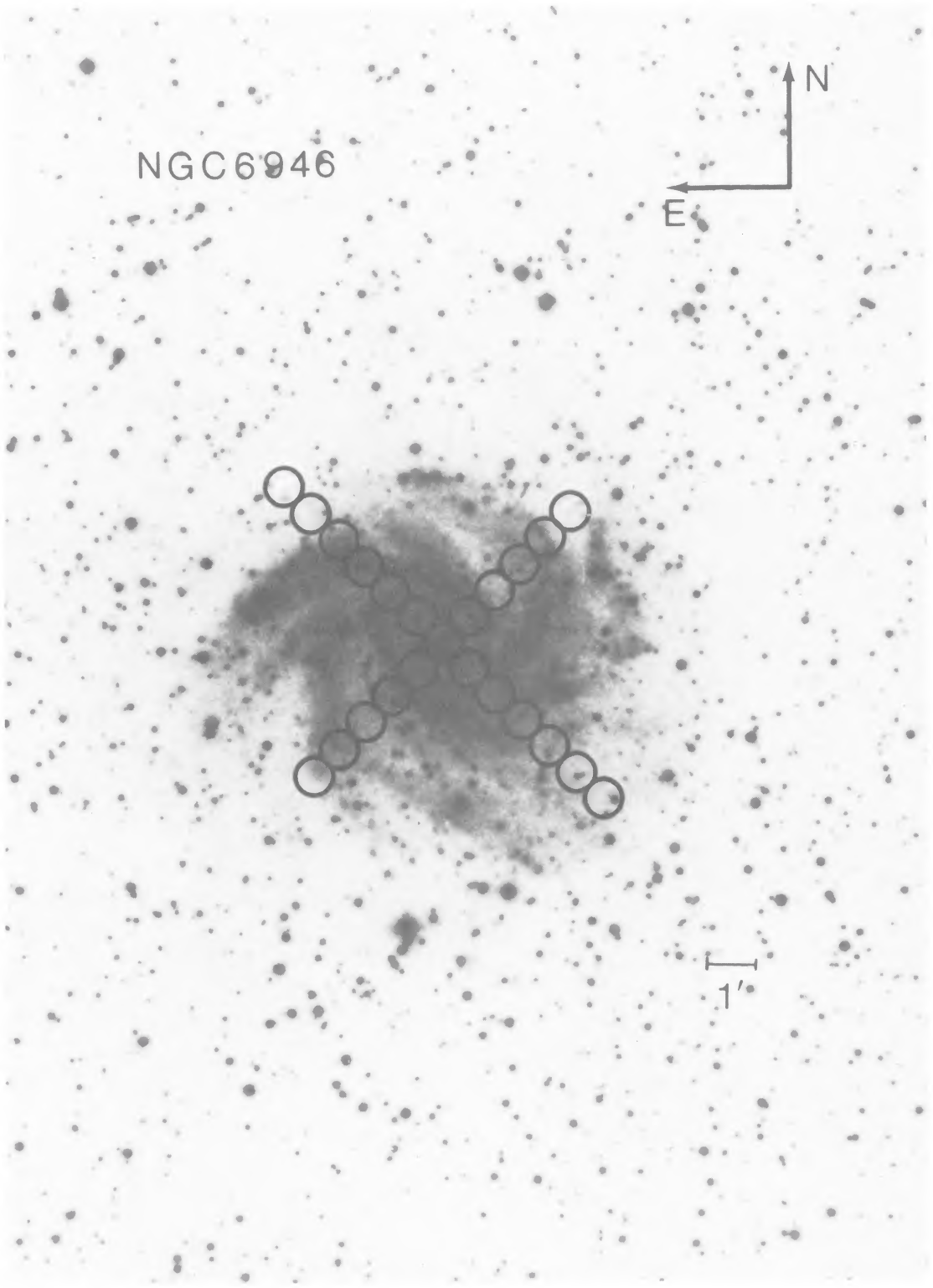

FIG. 1*b*

FIG. 1*b*.—Enlargement from blue Palomar Sky Survey plate of NGC 6946. Circles are 50″ in diameter (2.4 kpc) and represent positions where observations were made, spaced by 45″.

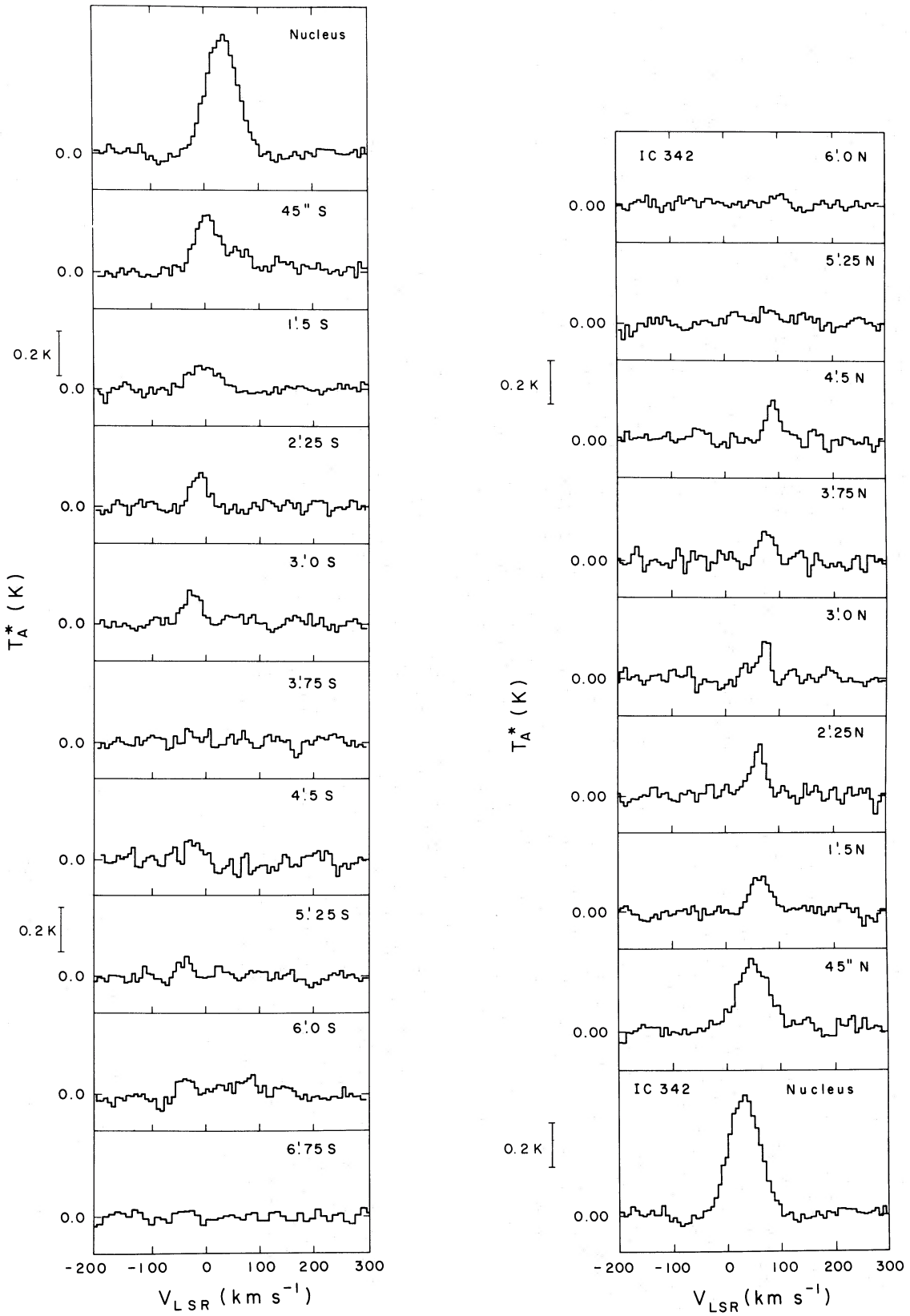

FIG. 2*a*.—Spectra of IC 342 along the north-south strip, indicated in Fig. 1*a*, smoothed to 7 km s^{-1} resolution. This strip is 40° from the major axis.

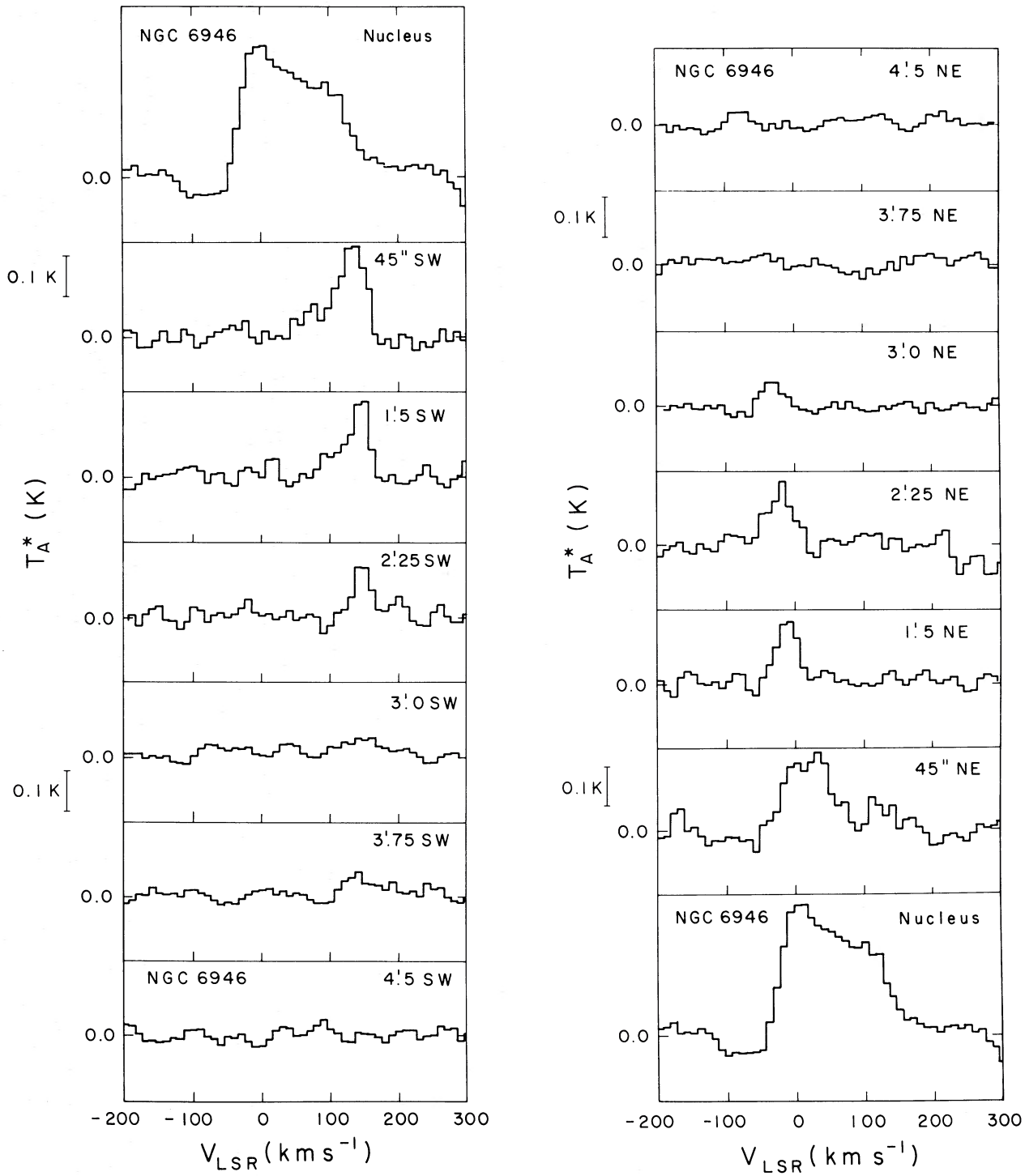

FIG. 2*b*.—Spectra of NGC 6946 along the northeast-southwest axis, indicated in Fig. 1*b*, smoothed to 10 km s^{-1} resolution. This strip is 17° from the major axis.

TABLE 2A

IC 342 LINE PARAMETERS

Position ($\Delta\alpha, \Delta\delta$) (unit = 45″)	T_A^{*}[a] (K)	I[a] (K km s^{-1})	V_{peak}[b] (km s^{-1})	V_{mean}[b] (km s^{-1})	ΔV (km s^{-1})	% Contrast Rel. to Exponential[c]
Center → North						
0,0	0.54	38.1	32	31	71	100
0,1	0.32	24.0	51	54	79	146
0,2	0.15	7.2	71	74	51	−5
0,3	0.20	7.2	67	58	41	22
0,4	0.14	4.9	78	64	34	7
0,5	0.13	4.0	80	79	33	14
0,6	0.18	6.1	90	95	35	123
0,7	0.06	2.5	85	81	41	17
0,8	0.05	1.6[d]	100	94	38	−4
Center → South						
0,0	0.54	38.1	32	31	71	100
0,−1	0.26	18.0	0	18	72	84
0,−2	0.11	6.8	−12	−4	65	−10
0,−3	0.15	5.3	−14	−15	35	−10
0,−4	0.14	5.4	−30	−26	38	19
0,−5	0.05	1.1	−34	−24	28	−69
0,−6	0.09	3.2	−34	−22	37	16
0,−7	0.08	2.2	−35	−33	29	3
0,−8	0.07	2.1[d]	−35	−30	24	26
0,−9	< 0.04	< 1.0	...	...	...	< −31
Center → East						
0,0	0.54	38.1	32	31	71	100
1,0	0.09	8.5	50	23	78	−11
2,0	0.14	5.4	75	55	38	−28
3,0	0.08	3.9	80	69	56	−34
4,0	0.05	2.7	70	66	49	−41
5,0	0.07	3.4	80	66	46	−4
6,0	0.05	2.2	85	58	30	−20
7,0	< 0.04	< 1.0	...	...	...	< −52
Center → West						
0,0	0.54	38.1	32	31	71	100
−1,0	0.18	13.3	10	11	77	39
−2,0	0.10	7.8	−10	−5	84	3
−3,0	0.05	1.7	−20	−18	33	−71
−4,0	0.08	3.0	−25	−32	42	−34
−5,0	0.08	3.4	−30	−28	38	−4
−6,0	0.14	3.0	−30	−24	19	9
−7,0	0.06	1.7	−30	−49	30	21
−8,0	0.04	< 1.0	...	...	...	< −41

external galaxies. Although our effective resolution (1 kpc and 2 kpc in IC 342 and NGC 6946) is clearly adequate, there is no evidence for a "hole" like that at $R = 1$–4 kpc between the nucleus and molecular cloud ring in our Galaxy. If there exists a gap in the molecular gas distribution in either external galaxy, it would have to be on a much smaller scale than our beam and would therefore not resemble the gas distribution in the Milky Way.

The CO emission as a function of radius is compared with the B luminosity profile observed for each galaxy (Ables 1971) in Figures 4*a* and 4*b*. The close agreement in the radial dependences is striking; *the* CO *distributions follow the luminosity profiles* in both galaxies. The

TABLE 2B

NGC 6946 LINE PARAMETERS

Position ($\Delta\alpha, \Delta\delta$) (unit = 32″)	T_A^*[a] (K)	I[a] (K km s^{-1})	V_{peak}[b] (km s^{-1})	V_{mean}[b] (km s^{-1})	ΔV (km s^{-1})	% Contrast Rel. to Exponential[c]
Center → Northeast						
0,0	0.33	46.4	50	53	133	50
1,1	0.20	14.8	20	35	86	3
2,2	0.16	6.3	−15	−8	43	−40
3,3	0.16	8.7	−20	−31	44	39
4,4	0.05	2.2[d]	−35	−30	39	−47
5,5	<0.04	<1.0	...	...	...	<−99
6,6	<0.04	<1.0	...	...	...	<−25
Center → Southwest						
0,0	0.33	46.4	50	53	133	50
−1,−1	0.22	16.5[d]	120	117	75	13
−2,−2	0.19	7.6	140	135	40	−16
−3,−3	0.12	4.4	140	156	32	−20
−4,−4	0.05	3.1	150	144	74	−4
−5,−5	0.06	3.4	140	155	53	42
−6,−6	<0.04	<1.0	...	...	...	<−25
Center → Northwest						
0,0	0.33	46.4	50	53	133	50
−1,1	0.10	12.2	60	54	126	−10
−2,2	0.10	11.2	55	67	107	31
−3,3	0.06	2.7	100	94	44	−64
−4,4	<0.06	<2.0	...	...	...	<−27
−5,5	<0.04	<1.0	...	...	...	<−45
Center → Southeast						
0,0	0.33	46.4	50	53	133	50
1,−1	0.21	26.7	60	62	126	50
2,−2	0.10	4.0	40	30	42	−93
3,−3	0.05	4.0	40	43	51	−10
4,−4	0.06	3.1[d]	40	41	50	18
5,−5	<0.03	<1.0	...	...	...	<−45

[a]Upper limits are 2 σ.
[b]Velocities are with respect to the Local Standard of Rest (LSR).
[c]% contrast given by eq. (2).
[d]Spectra obtained in marginal weather have 1 σ uncertainties of 1.0 K km s^{-1}.

luminosity profiles extend to 17 kpc (12.′5) in IC 342 and 23 kpc (8′) in NGC 6946, approximately twice as far out in radius as the CO distributions presented here.

The well-known exponential nature of the luminosity profiles is evident as a straight line in Figure 4. The observed CO radial distributions in both Scd galaxies are also fit well by an exponential distribution in R, where

$$I(R) = I_0 e^{-R/R_0}. \quad (1)$$

A least-squares fit of equation (1) to the data (excluding the nuclei plus seven points where $I_{CO} < 3\ \sigma = 1.5$ K km s^{-1}) yields $I_0 = 12.7$ K km s^{-1} and $R_0 = 4.1$ kpc for IC 342, and $I_0 = 23.4$ K km s^{-1} and $R_0 = 4.5$ kpc for NGC 6946. These exponential curves are superposed on the data in Figures 3*a* and 3*b*. Other functional forms were fitted to the data as well; in IC 342 both the exponential and a $1/R$ distribution give equally good fits at the 85% confidence level, which in NGC 6946 the data are fitted at the 75% confidence level by the exponential and by an $R^{-1.4}$ power law. Over the region where we have observed CO, it is therefore not possible to distinguish conclusively between an exponential and a power law. However, the luminosity profiles, which

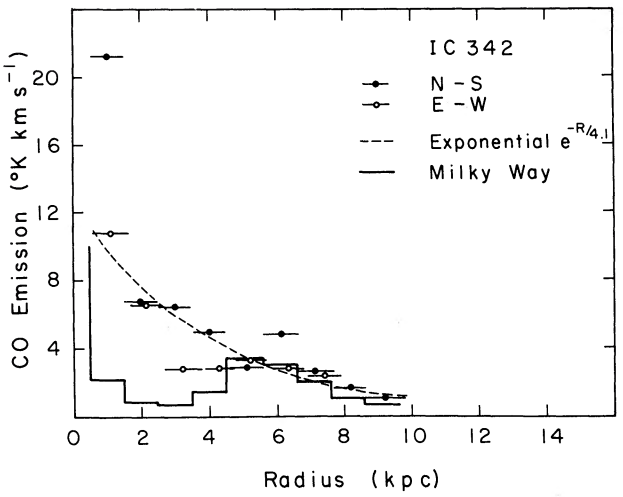

FIG. 3a

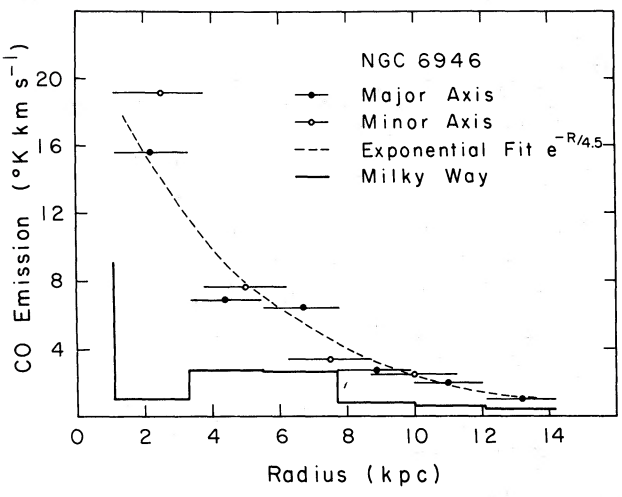

FIG. 3b

FIG. 3.—(*a*) CO radial distribution in IC 342. Filled circles represent the average emission at radii along the north-south strip; open circles represent the average emission along the east-west strip. The horizontal bars through the data points indicate the beam size on the galaxy. The solid line represents the CO distribution for the Milky Way viewed at the same inclination and distance as IC 342, and the dashed curve is the best exponential fit to the CO distribution. The nuclear emission in IC 342 (not shown) is off scale at 38.1 K km s^{-1}. (*b*) CO radial distribution in NGC 6946. Filled circles represent the average emission at radii along the northeast-southwest strip (17° from the major axis); open circles represent the average emission at radii along the northwest-southeast strip (17° from minor axis). The horizontal bars through the data points indicate the beamsize on the galaxy. The solid line represents the CO distribution for the Milky Way, viewed at the same inclination and distance as NGC 6946, and the dashed curve is the exponential fit to the CO distribution. The nuclear emission in NGC 6946 (not shown) is off scale at 46.4 K km s^{-1}.

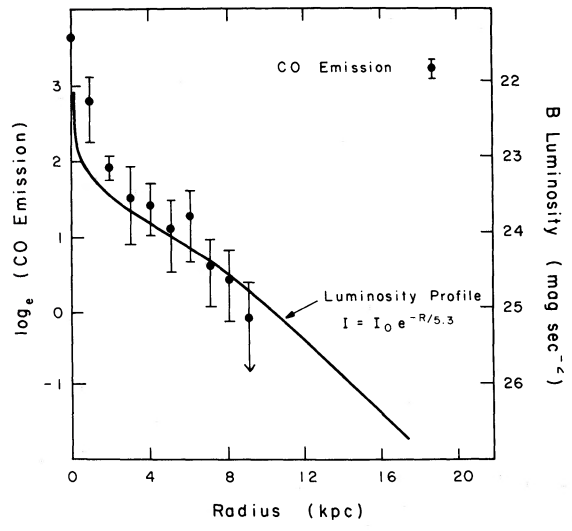

FIG. 4a

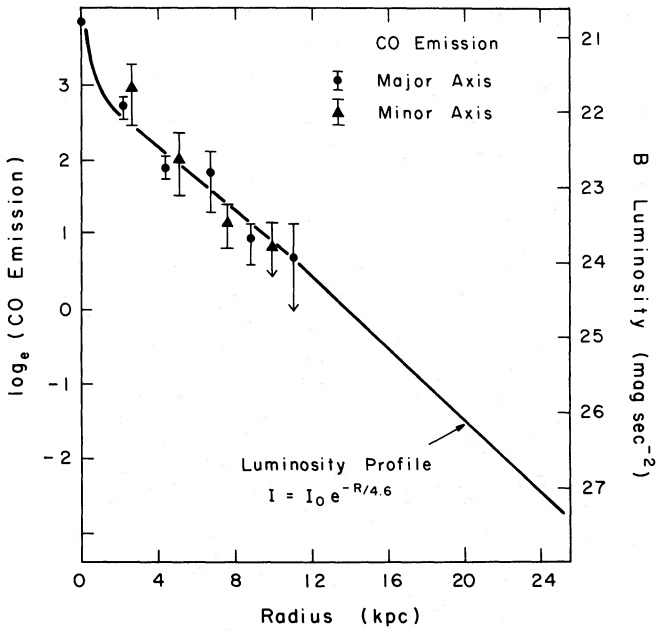

FIG. 4b

FIG. 4.—Comparison of the natural log of the CO emission with the B luminosity profiles of Ables 1971 for (*a*) IC 342 and (*b*) NGC 6946. The points plotted are the mean CO intensities at each radius, with bars indicating the spread in the observed intensities at each radius. The close agreement between the radial dependence of the CO emission and luminosity profiles is striking. The exponential nature of the luminosity profiles is evident on these semilog plots as a straight line. In the outer regions of the IC 342 where one of the measurements is an upper limit, the median rather than the mean is plotted. Where only one or two values were measured, with one upper limit, the mean is plotted as an upper limit.

extend twice as far in radius, clearly discriminate against a power law in favor of the exponential form. The particular functional form used to describe the distribution is not critical, since the important point is that the CO follows the light distribution.

In both galaxies the length scale R_0 for the falloff in CO *is in good agreement with that found previously for the disk component of the stars in these two galaxies* (Ables 1971). In IC 342 our least squares fit to the CO data gave $R_0 = 4.1$ kpc as compared with 5.3 kpc for the stellar disk. (An exponential fit excluding the strong positions 1 kpc N and S of the nucleus in IC 342 yields a scale length of 5.1 kpc). In NGC 6946 the exponential scale lengths are $R_0 = 4.5$ kpc for the scale CO data and 4.6 kpc optically. The length scales of 4–6 kpc found for the exponential disks in these two galaxies are typical of late-type spirals; a greater spread of 2–10 kpc for the scale lengths is seen in the earlier spirals (SO–Sbc) (Freeman 1970). In addition, nonthermal radio continuum observations of NGC 6946 are characterized by an exponential scale length of 4.7 kpc (van der Kruit, Allen, and Rots 1977), in agreement with the scale lengths for the cold gas and luminosity distributions. In fact this form also fits well the CO data in our Galaxy at $R = 5$–9 kpc (i.e., excluding the hole) with $I_0 = 17.3$ K km s^{-1} and $R_0 = 2.7$ kpc (Sanders, Solomon, and Scoville 1981).

The degree of clumping on the scale of our resolution (1–2 kpc) can be estimated from the fractional discrepancies of the observed individual intensities (not azimuthally averaged) relative to the exponential distribution in each galaxy. The percentage contrast between the observed values and the smooth distributions, defined by

$$C = \frac{I_{\rm obs} - I_{\rm exp}}{I_{\rm exp}} \times 100\% \qquad (2)$$

is given in the last column of Table 2 for each position. Including even the observations for which upper limits on the intensities were obtained, we find that only eight of 32 points in IC 342 and six of 22 points in NGC 6946 deviate by more than 40% from the smooth curves. Thus, in both galaxies, most of the observed intensities (excluding the nuclei) are close to an exponential distribution! The largest significant excursions from the exponential are two positions in IC 342 with contrast 100%–150%. One of these occurs in the dust arm 1 kpc N of the nucleus; the second occurs 6 kpc N of the nucleus at a position without especially strong optical emission or optical obscuration. The correlation of particularly strong or weak CO emission with optical features is discussed in § IV*e*.

b) *Kinematics of the* CO *Emission*

Figures 5*a* and 5*b* show the spatial velocity maps along two axes, north-south in IC 342 and northeast-

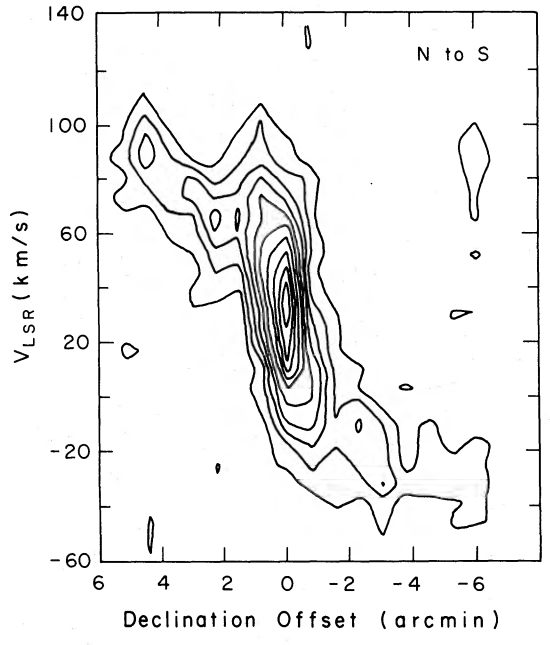

FIG. 5*a*

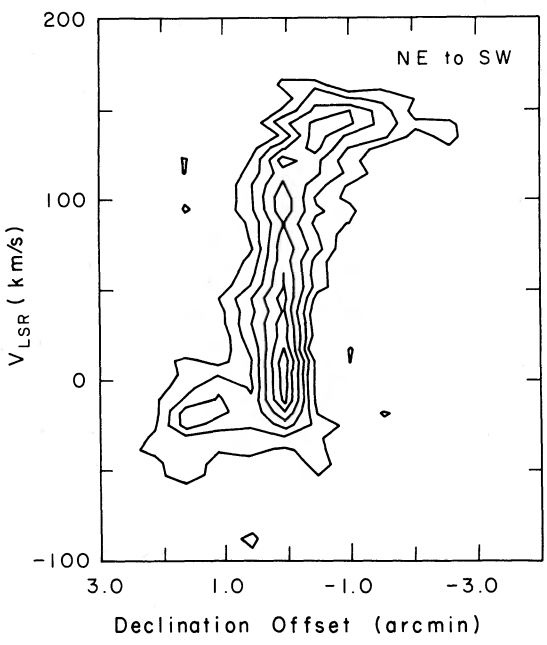

FIG. 5*b*

FIG. 5.—Observed rotational velocities (*a*) along north-south strip in IC 342 and (*b*) along northeast-southwest axis in NGC 6946. Contours are in intervals of 0.05 K.

TABLE 3

GALAXY PARAMETERS

Galaxy	IC 342	NGC 6946
R.A. (1950)[a]	$3^h\,41^m\,58^s.6$	$20^h\,33^m\,48^s.8$
Declination (1950)[a]	+67° 56′ 26″	+59° 58′ 50″
Systemic Velocity[b]	30 km s^{-1}	55 km s^{-1}
Distance[c]	4.5 Mpc	10.1 Mpc
Inclination[d]	25°	30°
Position Angle[d]	40°	62°
V_{max}[d]	192 km s^{-1}	208 km s^{-1}
Beam size on galaxy (50″)	1.1 kpc	2.4 kpc

[a] Positions are from Dressel and Condon 1976.

[b] Velocity relative to the Local Standard of Rest (LSR); these correspond to $V_{Sun} = 25$ km s^{-1} and 40 km s^{-1} for IC 342 and NGC 6946, respectively.

[c] For a summary of distance determinations, see text. Adopted distances are consistent with previous studies of these galaxies.

[d] Inclination, position angle of major axis and V_{max} are the same as those used by Rogstad and Shostak 1972.

southwest in NGC 6946. Since the major axis of IC 342 is at a position angle of 40°, both the north-south and east-west strips are nearly symmetrically placed with respect to the major axis. The major axis of NGC 6946 is at a position angle of 62°, so that the northeast-southwest strip is close to the major axis. The rotation of these galaxies is clearly evident from the shift of the peak velocities along the observed axes. The figures also illustrate dramatically the overall symmetry in kinematics about the nuclei.

We have derived CO rotation curves for these two galaxies at 50″ resolution assuming the same inclination, distance, systemic velocity, and position angle of the major axis as Rogstad and Shostak (1972) (see Table 3). Using the peaks of the CO emission lines as a function of radius, the velocities and radii were corrected for inclination and for the position angle of the observations. An uncertainty in the velocity of ±5 km s^{-1} in the line of sight translates to an uncertainty of ±15 km s^{-1} in the disk of IC 342 and ±10 km s^{-1} in NGC 6946, due to the nearly face-on aspects for both galaxies. The derived CO rotational velocities are shown in Figures 6*a* and 6*b* along with the H I rotation curves of Rogstad and Shostak. In both NGC 6946 and IC 342 the CO rotation curves are in good agreement with the H I data. As a further test of the validity of using peak velocities, we convolved the exponential CO distributions and H I rotation curves with a 50″ Gaussian beam. On the scale of our beam, the peak velocities expected at each radius were found to agree to within ±5 km s^{-1} with those determined from our observations. Optical rotation curves are not available for either of these galaxies.

Although the 50″ beam size limits our spatial resolution to 1 and 2 kpc for IC 342 and NGC 6946, respectively, one can use the velocity information contained in the nuclear spectra to deduce the gross features of the rotation curves within the inner 0.5 kpc of each galaxy, assuming smooth gas distributions. From the convolution of the Milky Way CO distribution and rotation curve with a 50″ beam scaled to the distances of the two external galaxies, the CO emission from the nucleus of our Galaxy can be compared with IC 342 and NGC 6946. The observed line profile for the nucleus of IC 342 is shown in Figure 7 along with that expected for the Milky Way at the same inclination. If IC 342 and NGC 6946 had rotation curves and gas distributions like the Milky Way, the central line profiles would have full widths at half maximum of ~220 and ~300 km s^{-1} respectively, as well as square shapes with "horns" at the extreme velocities in the profiles (see Fig. 7). We also present in Figure 7 the line profile expected at the nucleus of IC 342 based on the H I rotation curve, observed CO distribution, and random motions of 50 km s^{-1}. This profile more closely resembles the observed nuclear emission.[7] The results of this profile modeling support our conclusion that at 50″ resolution the rotation curves in IC 342 and NGC 6946, unlike that in our Galaxy, rise much more gradually to the peak rotational velocity. We cannot rule out the possibility, however, that there are rotational motions in the nuclei which are of the same order of magnitude as the random velocities included above, that is $V \sim 100$ km s^{-1} at 1 kpc in NGC 6946 and $V \sim 50$ km s^{-1} at 0.5 kpc in IC 342 (see § IV*d* for a derivation of the random velocity component of the line profiles).

c) ^{13}CO

The ^{13}CO observations were made at two positions in IC 342, on the nucleus and 6 kpc E of the nucleus. Figure 8 shows the CO and ^{13}CO spectra for the center of IC 342. The ratio of the CO to ^{13}CO peak intensities on the nucleus, is 8, whereas the CO and ^{13}CO integrated intensity ratio at this position is 11.7 due to the narrower width of the ^{13}CO line. Encrenaz *et al.* (1979) also measure a CO/^{13}CO ratio of 11.3 on the nucleus using an 88″ beam. The CO/^{13}CO intensity ratio of 11.7 measured in the nucleus of IC 342 is about a factor of 2 higher than is seen in typical giant molecular clouds in the Milky Way. Solomon, Scoville, and Sanders (1979) sampled 17 positions in the inner galactic plane at $b = 0°$ and found ratios for the integrated intensities ranging between 4 and 11 with a mean value of 6.2. At

[7] The asymmetric shape of the central profile in NGC 6946 suggests the presence of velocity asymmetries in the nucleus. Hα observations of J. Goad and J. Gallagher (1981, private communication) in the nucleus of NGC 6946 indicate that there is a giant H II complex 5″ from the nucleus with a velocity 50 km s^{-1} less than the systemic velocity; this region may be responsible for the asymmetry observed in the CO line profile.

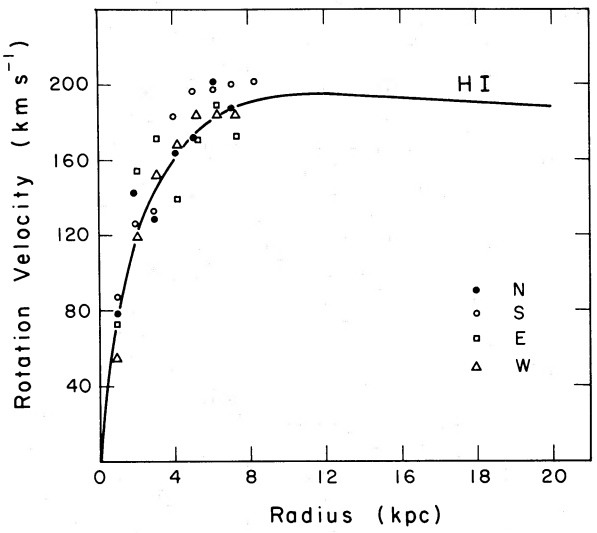

FIG. 6a

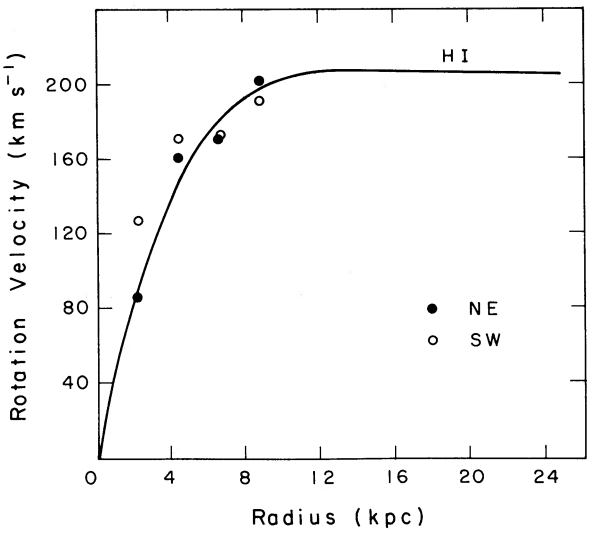

FIG. 6b

FIG. 6.—CO rotational velocities with 50″ resolution corrected to the plane of the galaxy for (*a*) IC 342 and (*b*) NGC 6946. The solid line indicates the H I rotation curve of Rogstad and Shostak 1972. In NGC 6946, only observations along the northeast-southwest axis (close to the major axis) contain velocity information for deriving the rotation curve.

the position of 6 kpc E the 2 σ limit on the integrated intensity ratio is > 7.

IV. DISCUSSION

a) *The Distributions of* H_2 *with Radius*

To obtain an H_2 mass estimate from the observed CO emission, we rely upon results from analysis of the CO emission in the Milky Way and assume a linear relationship between CO line flux and H_2 column density. Most previous analysis of extragalactic CO emission has relied upon the same assumption of linearity at least in regions outside the nucleus (e.g., Rickard *et al.* 1977 and Morris and Lo 1978), and an adopted constant of proportionality based on a single "standard" cloud which is thought to produce most of the emission. Rather than assume such a *single* standard cloud, we choose here to adopt a constant of proportionality based on *samples* of molecular clouds observed in our Galaxy.

In the Appendix we summarize the measured CO intensities and derived H_2 column densities obtained in regions ranging from the hot cores of giant clouds (e.g., Orion KL and M17SW) to nearby dark nebulae (e.g., the Lynds clouds) and a sample of 25 clouds selected from a uniform mapping of the inner galactic plane. Both the dark cloud and giant cloud samples yield similar empirical values for the *ratio* $\langle N_{H_2}/I_{CO}\rangle$, although the mean column densities within the two samples vary by a factor of 10. The latter sample is probably most applicable to analysis of the CO emission in external galaxies, since the 25 clouds came from an unbiased survey of the galactic plane at $l = 15°$–$35°$ with no preference to locate and observe either a particular cloud type or the centers of clouds. Based on this work, the empirical relations between the intensity integral and the inferred surface density of H_2 are

$$N_{H_2} \approx 4\times 10^{20} I_{CO} \cos i \quad H_2\ \mathrm{cm}^{-2} \tag{3a}$$

or

$$\sigma_{H_2} \approx 6 I_{CO} \cos i \quad M_\odot\ \mathrm{pc}^{-2}, \tag{3b}$$

where I_{CO} is the intensity integral (K km s^{-1}), and i is the galaxy inclination. The factor $\cos i$ corrects the column density to that which would be observed for a "face-on" galaxy. Adopting a constant of proportionality based on the hot core sources would increase the resulting mass estimates by a factor of five (see the Appendix). In any case, since the same constant of proportionality relating the CO line flux and H_2 mass density is used for the external galaxies and the Milky Way, the mass distributions should be correct at least in a relative sense assuming only a direct proportionality between the observed flux and the mass density averaged over the antenna beam. As discussed in the Appendix, the constant of proportionality relating CO to H_2 is uncertain by at least a factor of 2. This introduces an equivalent uncertainty into the abundance of H_2 relative to H I.

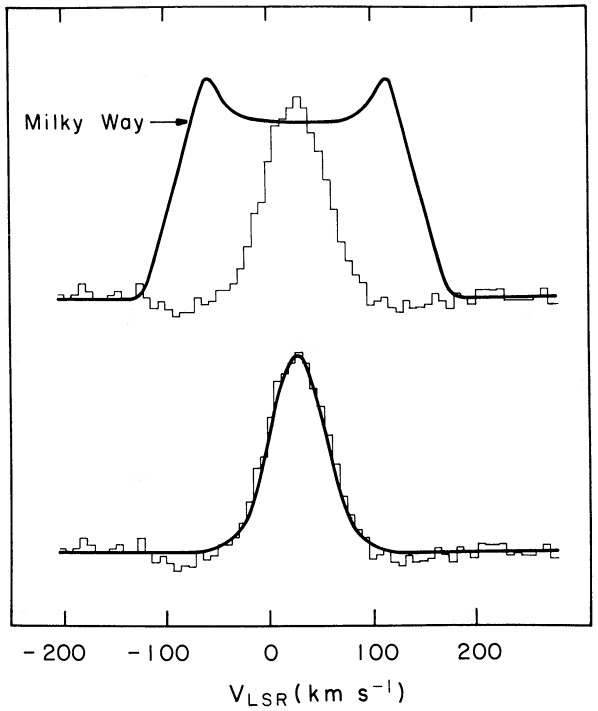

FIG. 7.—Comparison of the observed spectrum in the nucleus of IC 342 smoothed to 7 km s^{-1} resolution with (*upper*) the emission expected for the Milky Way with the distance and inclination of IC 342, derived from the convolution of the Milky Way rotation curve (Burton and Gordon 1978), a 50″ Gaussian beam, and CO distribution with a central peak and 5 kpc ring; and (*lower*) the emission expected for IC 342 from the convolution of the H I rotation curve (Rogstad and Shostak 1972) and the observed CO distribution with a 50″ Gaussian beam and velocity dispersion of 50 km s^{-1}. The observed profile shows no resemblance to the Milky Way emission, suggesting that the rotation curve for IC 342 does not have an inner bump like the Milky Way.

In Figures 9*a* and 9*b*, our derived H_2 mass distributions are shown together with the H I distributions from Rogstad and Shostak (1972). The most striking features shown are:

1. The abundance of H_2 far outweighs that of H I over 30%–40% of the optical disk, out to radii of 8 kpc in IC 342 and 10 kpc in NGC 6946;

2. The shapes of the H_2 and H I distributions diverge at $R < 10$ kpc. At small R, where the H_2 exhibits an exponential increase, the H I is either constant or decreasing with a hole at $R < 5$ kpc; and

3. The total density of interstellar gas (H I+H_2) is a strong function of galactic radius.[8]

In both galaxies (and indeed also in the Milky Way), the H_2 dominates over H I at the point where the *average* column density of hydrogen nuclei exceeds about 10^{21} cm^{-2}. The column densities in the external galaxies are averaged over the area of the beam; the actual column densities through the molecular clouds, which probably fill $< 2\%$ of the beam, must be much greater. The fact that the H_2 becomes dominant at a particular column density rather than at the same radius in all three galaxies suggests that conversion of H I to H_2 is determined by local conditions in the interstellar medium (e.g., the gas density) and not the large-scale galactic structure.

The fact that the CO emission follows the light is one of the most interesting features in the new data for IC 342 and NGC 6946. Although the origin of the exponential character of the stellar disk luminosity component has not been understood, our new data showing that the same distribution exists for the dense gas out to 10 kpc indicates that the *young* stellar disk may have this form because that is the *present* distribution of star forming material in the disk. In the model of Eggen, Lynden-Bell, and Sandage (1962) the disk is formed from gas left after the initial star formation during the collapse of the spherical protogalaxy. Freeman finds that the same exponential character exists in both the young and old stellar disk populations, implying that the exponential form of the disk gas "was defined during the settling phase of the disk, *before* significant star formation in the disk began." The more recent work of Schweizer (1976) indicates an exponential form in both the arm and disk components of the light distribution in several galaxies (e.g., M51 and NGC 4321). In summary, it would appear that not only do the young disk stars and gas have the same exponential distribution at present but a similar distribution probably existed in the past.

Most of the optical luminosity measured in the *B* band probably arises from comparatively young stars of age $< 2 \times 10^9$ yr. Barring the existence of *strong* extinction correlated with radius, the distribution of optical luminosity may therefore reflect the "recent" star formation rates at different radii. In order that extinction be a dominant influence on the radial light distribution, the extinction must be pervasive (i.e., covering more than 50% of the disk surface area). If the luminosity and H_2 distributions are indeed closely correlated in their radial dependences, this may be understood if the star formation rate varies approximately linearly with the

[8]This conclusion disagrees with Morris and Lo 1978 who suggested that the total density was approximately constant with radius. In the external galaxies our conversion between CO emission and derived H_2 column density would have to be off by a factor of ~ 20 before the total density (H I+H_2) would be constant. This factor far exceeds what we view as reasonable uncertainties in the relation between N_{H_2} and I_{CO} (see the Appendix). Based on an entirely different analysis, Rickard and Palmer 1981 derived a CO to H_2 conversion only a factor of 3 lower than that given in eq. (3). The effect of using this lower value is to move inward to ~ 5 kpc the radius at which H_2 dominates H I in these galaxies. The total density of ISM is still a strong function of radius, decreasing by a factor of 10 from the nucleus to the disk.

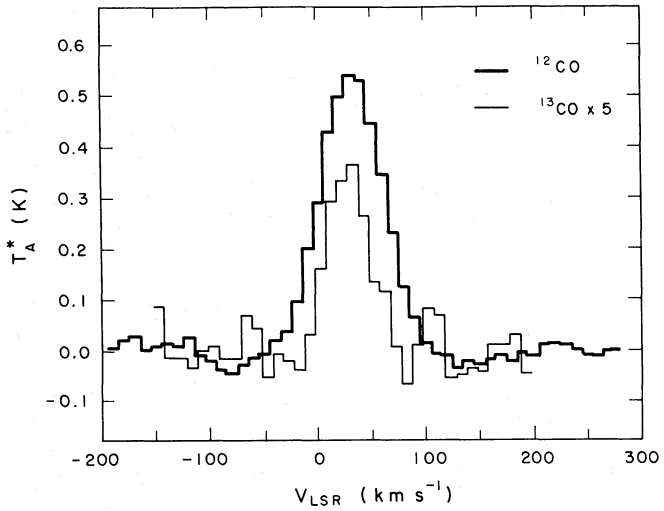

FIG. 8.—CO and ^{13}CO (times 5) in the nucleus of IC 342. The peak intensity ratio is 8, while the integrated area ratio is 11.7.

mean density and mass of H_2 and is relatively insensitive to external influences (e.g., galactic shocks or cloud-cloud collisions) which may be a strong function of galactic radius. Alternatively, *if* the ISM gas had, on the average, been cycled several times through stars, one would expect proportionality between the current rate of star formation and the density of gas. Assuming the stellar mass function does not change with time or radius in the disk (Searle, Sargent, and Bagnuolo 1973), this proportionality could be established because the ISM replenishment occurs from stars with $M > 2\ M_\odot$; the total mass density will then vary in direct proportion to the rate of star formation (i.e., the depletion process). Since it would take many cycle times to achieve such an

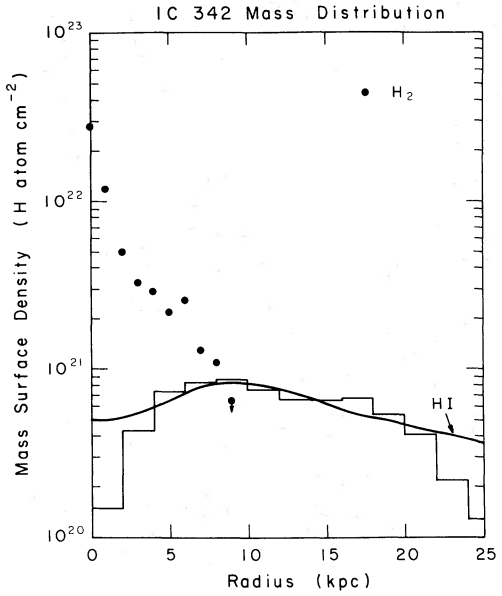

FIG. 9*a*

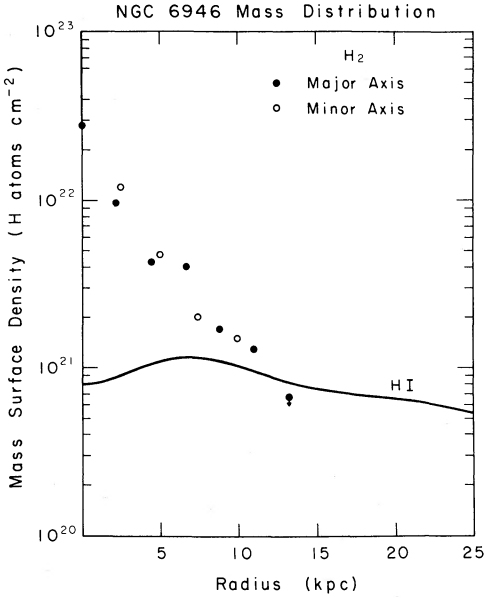

FIG. 9*b*

FIG. 9.—(*a*) Mass surface densities in IC 342. H_2 values are derived assuming a linear relationship between CO flux and H_2 mass (eq. [3a]). Filled circles represent H_2 derived from azimuthally averaged CO emission. The heavy curve represents the H I mass surface density from Rogstad and Shostak 1972, while the thin line histogram represents H I from Newton 1980*b*. H_2 dominates H I over the interior of the galaxy. (*b*) Mass surface densities in NGC 6946. H_2 values are derived assuming a linear relationship between CO flux and H_2 mass. The solid curve represents the H I mass surface density from Rogstad and Shostak 1972. H_2 dominates H I over the interior of the galaxy.

TABLE 4

MASS ESTIMATES FOR IC 342 AND NGC 6946

Parameter	IC 342	NGC 6946
CO Radius	8 kpc	11 kpc
$M(H_2)$	$4.1\times10^9\ M_\odot$	$1.1\times10^{10}\ M_\odot$
$M(H\ I)$	$1.2\times10^9\ M_\odot$	$3.6\times10^9\ M_\odot$
$M_{dynamical}$[a]	$6.5\times10^{10}\ M_\odot$	$1.1\times10^{11}\ M_\odot$
$M(H_2)/M_{dynamical}$[b]	0.06	0.10
$M(H\ I)/M_{dynamical}$	0.02	0.03
R_{25}	15 kpc	20 kpc
$M(H\ I)$	$4.1\times10^9\ M_\odot$	$8.6\times10^9\ M_\odot$
$M_{dynamical}$	$1.2\times10^{11}\ M_\odot$	$1.9\times10^{11}\ M_\odot$
$M(H_2)$[c]$/M_{dynamical}$	0.03	0.06
$M(H\ I)/M_{dynamical}$	0.03	0.05

[a] The dynamical mass is derived from the expression $M_{dyn}\approx 2.25\times10^5\ RV^2\ M_\odot$, where R is the radius in kpc at which the circular velocity is V in km s^{-1}.

[b] The two mass estimates M_{dyn} and $M(H_2)$ depend differently on the adopted distances; $M_{dyn}\propto d$ and $M(H_2)\propto d^2$.

[c] This is the H_2 mass within the CO radius and is thus a lower limit to the molecular fraction out to R_{25}.

equilibrium, we view the former explanation as more attractive.

b) *Mass of* H_2

Over the interiors of both IC 342 and NGC 6946, the abundance of molecular hydrogen greatly exceeds that of atomic hydrogen (Figs. 9*a* and 9*b*). We have determined the masses of H_2 in these galaxies by assuming azimuthal symmetry and summing over successive annuli, or

$$M(H_2)=\sum_{n=1}^{N}\sigma_n(H_2)A_n, \qquad (4)$$

where $\sigma_n(H_2)$ is the surface density derived for ring n, A_n is the area of ring n, and N is the number of different radii for which the surface density was determined. The H_2 mass in IC 342 out to 8 kpc is $4\times10^9\ M_\odot$, while that in NGC 6946 out to 12 kpc is $1\times10^{10}\ M_\odot$.

The H_2 mass estimates may be compared with those in H I (Rogstad and Shostak 1972) and the dynamical mass (stars + gas) obtained from the rotation curve. Over the regions where we have determined the integral H_2 masses in IC 342 and NGC 6946, the total mass of H_2 exceeds that of H I by a factor of ~ 3. It is not until one goes out to radii of 15–20 kpc that the interior masses of H I are comparable to the H_2 masses inside 10 kpc. The dynamical masses are derived from the rotation curve with the relation

$$M_{dyn}\approx 2.25\times10^5\ RV^2M_\odot, \qquad (5)$$

where R is the radius in kpc at which the circular velocity is V in km s^{-1}. Out to the radius defined by de Vaucouleurs as R_{25} (the radius at which $B=25$ mag arcsec^{-2}), H_2 and H I each consist of 3% of the dynamical mass in IC 342. In NGC 6946 H_2 is more abundant, comprising 6% of the dynamical mass out to R_{25},[9] compared with 5% for H I. These mass estimates are summarized in Table 4.

c) *On the Absence of "Rings"*

One of the most remarkable features of the H_2 (and H II) distribution in the Milky Way is the maximum in the form of a ring at radii 4–8 kpc. The spatial resolution of our observations in IC 342 and NGC 6946 is 1–2 kpc, and both galaxies are seen nearly face-on; it is therefore clear that if such a ring were present in these galaxies it would have been easily detected. The absence of a "ring" in both of the Scd galaxies can provide important clues to its origin in our own Galaxy.

Preliminary to our discussion, we assert that the actual discrepancy in the H_2 distributions in the three galaxies occurs at *1–4 kpc as a relative deficiency of gas in our Galaxy* rather than at 4–8 kpc in the form of an excess, i.e. the ring. This is established by the data showing all three galaxies with similar exponential falloffs in the gas disks at $R>5$ kpc. On the other hand, neither of the external galaxies has a local minimum inside 5 kpc, only a continuous rise in surface density towards the nucleus.

A key to understanding the paucity of interstellar matter in the Milky Way between 1 and 4 kpc is provided by comparison of the rotation curves of the Milky Way, IC 342, and NGC 6946 (Fig. 10). The most notable difference in the rotation curves is the extent of the "solid body" portion ($V\propto R$) occurring in these galaxies. With 50″ resolution in both IC 342 and NGC 6946 the circular velocity rises relatively slowly to a maximum at $R\approx10$ kpc; the solid body portion thus extends out to $R\approx5$ kpc in these two galaxies. In the Milky Way the rise is much steeper, with the initial maximum occurring within 1 kpc of the nucleus. Despite the uncertainty in the determination of the rotation curve in the inner 4 kpc of our Galaxy where there are clear radial motions, the rigid body rotation in the Milky Way extends over a much smaller region than in the two external galaxies (see § III*b* for a discussion of the rotation curves in IC 342 and NGC 6946).

The difference in the rotation curves is significant in predicting where the inner Lindblad resonance (ILR) will occur in the three galaxies. This resonance arises when the natural frequency κ for radial oscillations about the circular orbit (i.e., epicyclic motion) is com-

[9] These are the H_2 masses determined within the radius of the CO observations, and are therefore lower limits to the molecular gas fraction within R_{25}.

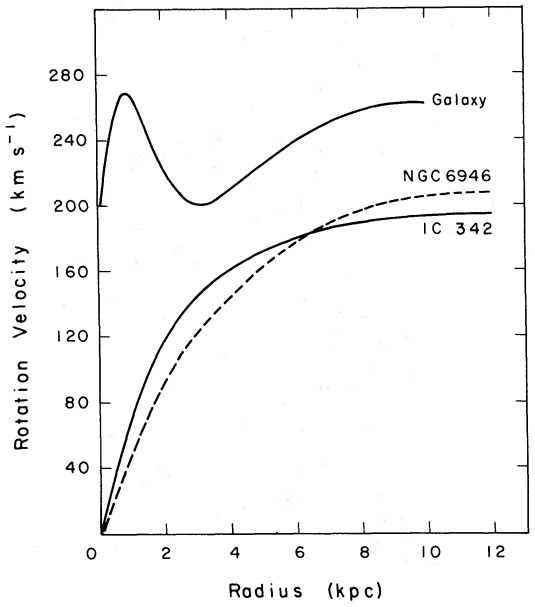

FIG. 10.—Rotation curves of IC 342 and NGC 6946 (Rogstad and Shostak 1972) compared with that for the Milky Way (Burton and Gordon 1978). In IC 342 and NGC 6946 the roughly solid body rotation extends to ~ 5 kpc, while in the Milky Way the solid body rotation occurs only for the inner 1 kpc. The inner Lindblad resonance in the Milky Way might be expected at $R = 2$–4 kpc.

mensurate with the frequency of radial excitations by the two arm spiral density wave. If the inner resonance occurs at all, it must be outside the region of nearly solid body rotation. One therefore expects the ILR will occur at $R = 2$–4 kpc in our Galaxy but probably not at all in IC 342 and NGC 6946 (cf. Kormendy and Norman 1979). Gordon (1978) *assumed* that the ILR in the Milky Way occurs at 4 kpc, on the edge of the molecular ring, and thereby derived the spiral pattern speed in our Galaxy.

Since the density wave tends to feed energy into the random motions of the stars and gas at the ILR, the effect of this resonance could be to remove any interstellar gas which may have existed originally at $R = 2$–4 kpc in our Galaxy to either larger or smaller radii. That is, as the gas from this zone executes large radial oscillations, it would collide with gas clouds at larger and smaller radii. Although some of the kinetic energy in this radial motion would be dissipated, the angular momentum of the colliding gas columns would be shared and conserved. As a result the gas originally in the ILR zone would no longer return to the equilibrium radius from which it started but would preferentially remain at larger or smaller radii depending upon whether it collided with gas on the exterior or interior portion of its epicyclic motion. Sanders (1979) has performed numerical calculations which attempt to model the inward flow of gas due to the high "viscosity" occurring at $R = 4$ kpc in our Galaxy and finds a depletion in the region between 1–4 kpc like that which is observed.

Alternatively, the presence of a hole in the gas distribution could be related to the history of star formation in the galaxy rather than to dynamical processes at the ILR. During the collapse of a protogalaxy, the formation of a large nuclear bulge could use up much of the gas in the interior and leave a hole in the overall gas distribution. The presence of a nuclear bulge mass is evidenced by an inner bump in a galaxy's rotation curve. The smooth rotation curves of IC 342 and NGC 6946 are consistent with small nuclear bulges, and the observed H I+H_2 gas distributions increase continuously in toward the centers. In this scenario the gas in IC 342 and NGC 6946 is in molecular clouds rather than having been exhausted in stars in a nuclear bulge.

As a test of the hypothesis that the deficiency of gas at $R = 1$–4 kpc in the Galaxy is related to either the presence of a bulge or a disturbance at the ILR, we have briefly observed the ScI galaxy NGC 4321 (M100). This galaxy has a steeply rising rotation curve with a dip from 1–2 kpc (Rubin, Ford, and Thonnard 1980) similar to the Milky Way (Fig. 11*a*). At a distance of 20 Mpc, our angular resolution of 50″ corresponds to 5 kpc on NGC 4321, and we cannot therefore expect to clearly resolve a hole (if it exists) between the nuclear and disk components. We can, however, compare the CO radial distribution observed in NGC 4321 to that in the Milky Way smoothed to a resolution of 5 kpc.

In NGC 4321, spectra were obtained at seven points spaced by 45″ in the east-west direction; the nuclear spectrum is shown in Figure 11*b*. Since similar integrated intensities were measured at positions symmetric about the center, we plot in Figure 12 the average CO intensity at each radius. Also shown in Figure 12 is the CO distribution for the Galaxy smoothed to 5 kpc resolution. For the Milky Way, the emission from the nucleus is 1.3 times stronger than the emission at 5 kpc, while in NGC 4321 the nucleus is 1.1 times the emission at 5 kpc. In contrast, the observations of IC 342 smoothed to 5 kpc resolution indicate that the emission from the nucleus would be 3 times the intensity at 5 kpc. The H_2 distribution in NGC 4321 thus bears much closer resemblance in form to that in Milky Way than to that in IC 342.

Photometry of NGC 4321 (Schweizer 1976) indicates that the luminosity profile of this galaxy is exponential between 5 and 20 kpc with a scale length of 6.3 kpc, compared with 5.8 kpc derived from our observations between 3 and 15 kpc. The mean *B* magnitudes which Schweizer presents for this galaxy show a significant *decrease* in the surface brightness distribution of the arm component at $R < 5$ kpc (see Schweizer 1976, Fig. 7). The bump in the rotation curve of NGC 4321 suggests the presence of a small nuclear bulge, and the gas distribution in this galaxy does not increase as continu-

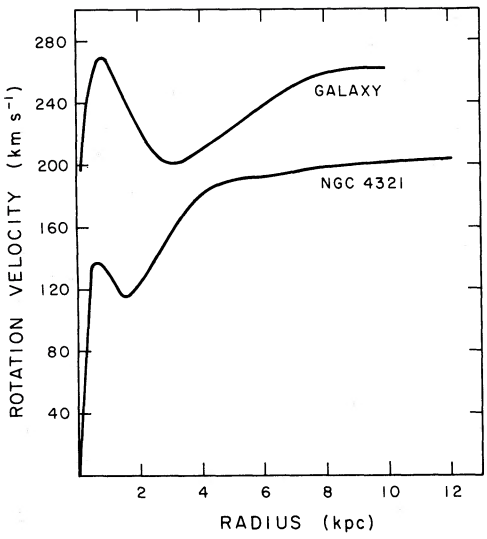

FIG. 11*a*

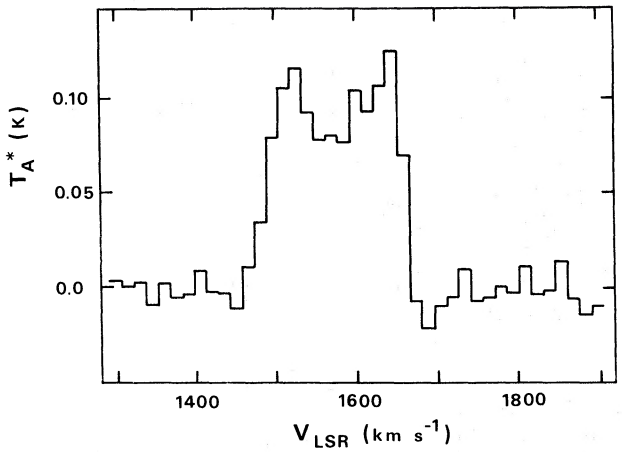

FIG. 11*b*

FIG. 11.—(*a*) Rotation curve of NGC 4321 determined from optical observations (Rubin, Ford, and Thonnard 1980), compared with that of the Galaxy. Both galaxies have inner bumps at $R \sim 1$ kpc. (*b*) Spectrum of CO emission in the nucleus of NGC 4321 smoothed to 15 km s^{-1}. The 50″ beamsize on this galaxy corresponds to ~ 5 kpc.

ously into the center as do those in IC 342 and NGC 6946.

At present it is not possible to determine whether it is the formation of the nuclear bulge which leaves a hole in the gas distribution or the disturbance at the ILR which creates the hole. Observations of CO radial distributions in nearby galaxies with large nuclear bulges are necessary to help resolve this question.

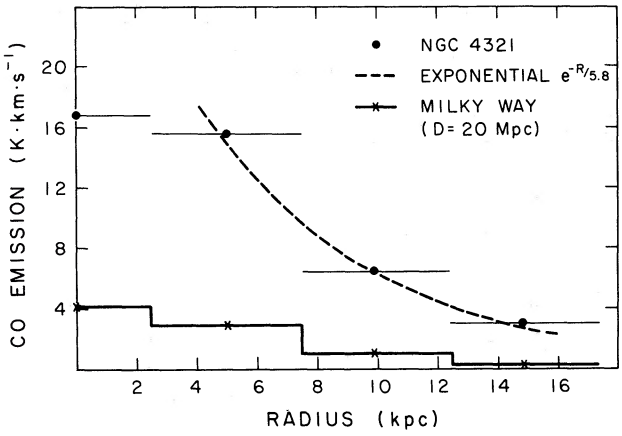

FIG. 12.—CO radial distribution in NGC 4321. Filled circles represent the average emission at radii along the east-west strip. At a distance of 20 Mpc, the beamsize corresponds to 5 kpc on the east-west axis of the galaxy—horizontal bars through the data points indicate the beamsize. The solid line represents the CO distribution which would be observed for the Milky Way at a distance of 20 Mpc and an inclination of 35°. The dashed curve represents the best exponential fit to the CO distribution. Unlike IC 342 and NGC 6946, the NGC 4321 nuclear emission with 5 kpc resolution does not greatly exceed the disk emission.

d) *Kinematics of Molecular Clouds*

Both random and organized motions of the molecular gas in the disk of a galaxy contribute to the widths of the observed spectral lines. In order to compare the observed line widths with those expected from pure rotation, we have convolved the observed exponential CO distributions and smooth H I rotation curves with a 50″ Gaussian beam. The velocity widths expected from the orbital motions included in the beam ($\Delta V_{\rm rot}$) are compared with the observed line widths ($\Delta V_{\rm obs}$) in Table 5. Typically, the observed widths far exceed those expected from circular motions, suggesting that much of the velocity broadening must be due to random cloud motions (or departures from the smooth rotation curves). The discrepancies are particularly clear in IC 342; Table 5A indicates that $\Delta V_{\rm obs}$ is a factor of 2–3 higher than $\Delta V_{\rm rot}$ at *all* positions. Although the large random velocities are less clear cut in NGC 6946 due to the larger beam size on this galaxy (and the consequently greater rotational broadening), it is still evident that the minor axis (northwest-southeast) shows systematically broader lines by $\sim 50\%$ than are expected from galactic rotation.

If we define the line width due to random motions ($\Delta V_{\rm random}$) as $\Delta V^2_{\rm random} = \Delta V^2_{\rm obs} - \Delta V^2_{\rm rot}$, then it is possible to determine the magnitude of these motions as a function of radius in NGC 6946 and IC 342. The random motion line widths are also listed in Table 5. In both galaxies the calculated random velocities are great-

TABLE 5A

OBSERVED AND MODEL LINE WIDTHS IN IC 342

R (kpc)	ΔV_{rot}[a] (km s^{-1})	ΔV_{obs}[b,c] (km s^{-1})	ΔV_{random}[b,c] (km s^{-1})
	North-South		
0	28	71	65
1	30	75	69
2	21	58	54
3	16	38	34
4	14	36	33
5	13	30	27
6	12	36	34
7	10	(35)	(33)
8	10	(31)	(29)
	East-West		
1	31	77	70
2.....	22	61	57
3	18	44	40
4	16	45	42
5	14	42	39
6	12	26	23

TABLE 5B

OBSERVED AND MODEL LINE WIDTHS FOR NGC 6946

R (kpc)	ΔV_{rot}[a] (km s^{-1})	ΔV_{obs}[b,c] (km s^{-1})	ΔV_{random}[b,c] (km s^{-1})
	Northeast-Southwest		
0	56	133	121
2.2	61	72	38
4.4	36	42	22
6.7	23	38	30
8.9	17	(56)	(53)
	Northwest-Southeast		
2.5	58	126	112
5.0	48	74	56
7.5	37	45	26
10.0	29	(50)	(41)

[a]The line width (FWHM) attributable to galactic differential rotation over the area of the beam. This estimate was obtained by convolution of the 50″ beam with a model galaxy having the observed intensity distribution (exponential with radius) and the observed rotation law.

[b]The parentheses indicate those positions with low signal-to-noise ratios, for which the line width is not a good measure of random motions.

[c]The component of the observed line width due to random motions, as opposed to rotational motion, is calculated from: $\Delta V_{random} = (\Delta V_{obs}^2 - \Delta V_{rot}^2)^{1/2}$.

est in the nuclei ($\Delta V_{random} = 70$–130 km s^{-1}) and decrease typically to ~ 30 km s^{-1} at $R > 4$ kpc.

Measurements of the gas velocities in our own Galaxy at $R > 4$ kpc indicate that random motions *in the disk* are characterized by $\Delta V_{FWHM} \approx 9$ km s^{-1} (i.e., a dispersion $\sigma_v \approx 4$ km s^{-1}; Burton and Gordon 1978) which is a factor of 3–4 less than the estimated ΔV_{random} in IC 342 and NGC 6946. Since the two galaxies observed here are seen nearly face-on ($i \approx 30°$), the observed widths necessitate $\Delta V = 60$–80 km s^{-1} in the disk. For this reason we believe it more plausible that the line widths are in fact due to harmonic motion in the Z-direction. Indirect estimates of the velocity dispersion in the Z-direction in the Milky Way by analysis of scale height data for CO yield values $\sigma_{v_Z} = 4$–9 km s^{-1} with implied $\Delta V_{FWHM} = 9$–22 km s^{-1} in Z (Stark 1979). Thus it would appear that the random motions we find in the external galaxies are probably a factor of 2–3 higher than those in the Milky Way both in the plane and in Z. They are not, however, inordinately large compared to the velocity dispersions obtained from Hα studies of H II regions in external galaxies. In M33 and M101 Smith and Weedman (1970, 1971) find $\sigma_v = 19$ km s^{-1} and in the disk of M51 Tully (1974) found $\sigma_v = 17$ km s^{-1}, corresponding to $\Delta V_{FWHM} \approx 42$ km s^{-1}. In the LMC Smith and Weedman measured $\sigma_v = 11$ km s^{-1}.

If in fact the line widths are due to Z-motions, the observed ΔV is related directly to the scale height of the H_2 gas clouds and the mass density of stars close to the disk. Assuming the H_2 gas in the two galaxies has the same thickness in Z as the Milky Way ($\Delta Z_{FWHM} \approx 130$ pc; Cohen and Thaddeus 1977; Solomon, Sanders, and Scoville 1979), we find the total mass density required for $\Delta V_{random} = 30$ km s^{-1} is the equivalent of $n_H = 45$ cm^{-3} at $Z = 0$. This mass presumably in stars, is 5–10 times the mass density in the H_2 gas found in the disks of these external galaxies (§ IV*a*).

In the nucleus of the Milky Way large noncircular motions ($\Delta V \approx 50$–150 km s^{-1}) are observed in the molecular gas (cf. Scoville, Solomon, and Jefferts 1974). By analogy with our own Galaxy, it is therefore possible that the large line widths seen in the nuclei of IC 342 and NGC 6946 have a similar origin and are not Z-motions as we believe to be the case at $R > 4$ kpc.

e) *Spiral Structure*

Although spiral structure is obvious optically in many disk galaxies, studies of the luminosity profiles of spiral disks have shown that the light distributions decrease exponentially with radius (Freeman 1970; Schweizer 1976; Boroson 1981). Schweizer's observations indicate that the scale length of the "disk and arms" in galaxies with well developed spiral structure is slightly larger than that of the "disk" alone. Boroson (1981) has shown that departures from exponential distributions tend to occur when there has been recent star formation in the disk. These results suggest that the spiral pattern is a perturbation superposed upon the underlying exponential distribution.

Currently, the question as to whether molecular clouds are confined to spiral arms in our own galaxy remains

unanswered (Blitz and Shu 1980; Cohen *et al.* 1980; Sanders, Solomon, and Scoville 1981). Thus, observations of external galaxies with sufficient resolution, sensitivity, and coverage are crucial for addressing the question of molecular cloud location vis à vis the spiral arms. The observations presented in this paper indicate that the CO radial distributions are well-described by an exponential in IC 342 and NGC 6946. However, there are small deviations from the exponential which may correlate with spiral features. One difficulty in determining if CO emission is enhanced along spiral features arises in locating precisely where the arm and interarm regions lie. Although in IC 342 the 50″ beam size is comparable to the interarm spacing, the spiral structure is sufficiently patchy to make the problem of arm location quite complex, a conclusion also reached by Morris and Lo (1978). Since NGC 6946 has a smaller angular size than IC 342, the telescope beam averages over a larger region with respect to the arm–interarm spacing

In order to investigate the existence of any correlation between the observed emission and spiral features, we have considered the positions which show the largest departures from the exponential distribution, and compared these positions with Ables's (1971) luminosity profiles and optical photographs of the galaxies. Although several correlations were found between optical features and strong CO emission (see following discussion) there are many additional optical features for which enhanced emission is not present.

In the last column of Table 2 we list the contrast factor (C) as the % deviation of the observed emissivity from the exponential distribution. In IC 342 the largest positive deviations from the exponential ($C > 80\%$) occur in the nucleus, one beam N, six beams N and one beam S of the nucleus. In the inner 1 kpc of IC 342, dust lanes are present to the north and south of the nucleus (Morris and Lo 1978). Thus, it is likely that the enhanced CO emission observed correlates with the dust lanes near the nucleus. The position six beams N of the nucleus is located on one of the spiral arms; the position five beams N is also on an optical arm, but does not exhibit the enhanced emission seen at the neighboring position.

In IC 342, more CO emission was detected in the north-south direction than east-west. In the east, the intensities are all deficient relative to the exponential.[10] The most significant deficiencies in IC 342 ($C < 50\%$) are found five beams S and three beams W of the nucleus. Neither of these positions is located between arms, and both have some associated optical emission.

In NGC 6946 the contrast factors span a smaller range of values, probably due to the much lower spatial resolution. The largest positive deviations ($C > 35\%$) are found in the nucleus, three beams NE, one beam SE, and five beams SW of the nucleus. To the northeast, there is a prominent spiral arm which has been detected in CO (Morris and Lo 1978). The position we observed three beams to the NE is located on this arm, and shows enhancement relative to the exponential distribution. The position one beam SE of the nucleus also shows enhanced emission relative to the exponential, coincident with a prominent dust lane and spiral arm 2 kpc from the center. To the southwest of the nucleus, there is low lying CO emission five beams away. Ables's (1971) luminosity profile for NGC 6946 along the major axis (axis 1 in that study) shows an optical feature at this SW position where we see excess emission.

The two positions in NGC 6946 where the CO emission is deficient relative to the exponential by more than 75% are five beams NE and two beams SE. The position to the northeast is past the prominent optical arm. Ables's luminosity profile in this region shows a sharp falloff at roughly the position where we see very little emission. The position two beams to the SE is just outside the bright nuclear region where the optical luminosity is decreasing rapidly with radius (Ables's axis 2).

Although it is possible to correlate the observed CO enhancements with dust lanes or luminous spiral arms, the presence of such optical features does not always guarantee strong CO emission. Conversely, deficiencies in CO do not always correlate with interarm regions. These observations suggest that the CO is not confined solely to the spiral arms but is distributed throughout the disks in both galaxies. The spiral arms may then result from stochastic star formation processes (Seiden and Gerola 1979) or from an increase in the efficiency to trigger star formation by density waves in the arms as compared with other areas.

V. CONCLUSIONS

The principal conclusions of our observations in the two late-type spiral galaxies are:

1. In both IC 342 and NGC 6946 the CO radial distributions out to $R \approx 10$ kpc follow the exponential luminosity profiles with scale lengths of 4 kpc. The CO emission in IC 342 and NGC 6946 does not exhibit the central peak and ring structure of the Milky Way.

2. The mass density of H_2 dominates H I over 30%–40% of the optical disk. In IC 342 the total mass of H_2 out to $R = 8$ kpc is $4 \times 10^9\ M_\odot$; in NGC 6946 the total mass of H_2 out to $R = 12$ kpc is $1 \times 10^{10}\ M_\odot$.

3. Several positions showing strong CO emission relative to the exponential distribution are associated with specific optical features—emission regions and dust lanes. However, there are also many positions with strong CO emission having no obvious optical associa-

[10] We note that the exponential scale length for the east-west points in IC 342 is similar to that for the north-south points, but the absolute intensities are slightly lower along the east-west axis.

tion. Global spiral structure is therefore not evident from the molecular data.

The extragalactic CO observations reported here also provide important insight for understanding the molecular distribution in our own Galaxy:

1. The deficiency of molecular gas between 1 and 4 kpc from the galactic center is possibly due either to action of the inner Lindblad resonance (ILR) which occurs in this zone or to the presence of a nuclear bulge. This explanation is consistent with the greater continuity seen in the CO distributions in NGC 6946 and IC 342 which have small bulges and where no ILR is expected (as inferred from their rotation curves).

2. The exponential dependence of the CO emission at $R = 5$–9 kpc in the Milky Way strongly supports the picture in which H_2 is dominant over H I in this region. In the two external galaxies where H_2 clearly dominates H I, we also find the H_2 distribution mimicking the exponential distribution of the stellar disk, indicating that the star formation rate per nucleon is constant.

We wish to thank Drs. V. C. Rubin, R. B. Tully, A. Bosma, R. Giovanelli, and J. Weisberg for helpful discussions; and L. Tacconi and P. van West for help with the observations. This is contribution 484 of the Five College Astronomy Department. N. Scoville is grateful to the University of Hawaii for a sabbatical leave appointment.

APPENDIX

RELATING CO LINE FLUX TO MOLECULAR COLUMN DENSITY

In this Appendix we examine observational data for various clouds observed in our Galaxy to derive an *empirical* curve of growth relating observed CO intensity integrals to the H_2 column density obtained from either extinction estimates, ^{13}CO measurements, or virial theorem analysis.

We consider as a representative range of CO emission regions: (1) the hot core regions observed in a few clouds such as Orion, (2) nearby dark nebulae (observed by Dickman 1978 and Frerking, Langer, and Wilson 1982), and (3) a sample of giant molecular clouds sampled from a survey of the inner galactic plane (Solomon, Scoville, and Sanders 1982). In Table 6, we have tabulated the CO intensities I_{CO} (K km s^{-1}), the intensity ratio $I_{CO}/I_{^{13}CO}$, H_2 column densities, and last, the ratio N_{H_2}/I_{CO} for these sources. All CO intensities were reduced to a common brightness temperature scale adopted by Ulich and Haas (1976) at NRAO.

The H_2 column densities used in this analysis are from numerous sources. For the dark nebulae the H_2 column densities were determined from visual and IR extinction estimates assuming a standard gas-to-dust ratio $N_{H_2}/A_v = 0.94 \times 10^{21}$ cm^{-1} mag^{-1} (Bohlin, Savage, and Drake 1978). In the cloud cores N_{H_2} was derived from LTE analysis of ^{13}CO and CO data and an abundance ratio $(H_2/^{13}CO) = 10^6$ appropriate to $A_v > 4$ mag (Frerking, Langer, and Wilson 1982). The best estimate of the $(H_2/^{13}CO)$ abundance ratio determined by Dickman (1978) is 5×10^5, but this value applies to clouds with $A_v \leq 2$ mag. In the galactic plane sample of Solomon, Scoville, and Sanders (1982), column densities in 25 clouds were estimated from the line widths and sizes using the virial theorem, and a more limited sample of 15 was also measured in ^{13}CO. The two methods agree within 30% for a fixed abundance ratio $(H_2/^{13}CO) = 10^6$.

From the last column of Table 6 it is evident that the derived N_{H_2}/I_{CO} values are similar. Excepting the positions of hot cores in molecular clouds we find an approximately constant value for the ratio of $N_{H_2}/I_{CO} \approx 4 \times 10^{20}$ cm^{-2} (K km s^{-1})$^{-1}$. Thus over a set which includes dark nebulae with $\langle A_v \rangle \approx 2$ mag and giant clouds with $\langle A_v \rangle \approx 22$ mag, the range in the ratio is only $\sim 40\%$ which is within the dispersion found for the points in each individual sample. It is unlikely that this constancy is fortuitous since the H_2 column densities in the different samples were obtained by independent techniques (extinction, virial theorem, and ^{13}CO analysis) and involved three different observing groups. For the giant cloud sample, both ^{13}CO and virial theorem estimates were in good agreement. If we take the variation in the empirical ratio N_{H_2}/I_{CO} from one sample to another (or the dispersion within each sample) as indicative of the uncertainties in the derived N_{H_2} we must conservatively take the mass estimates in the external galaxies to be uncertain by at least a factor of 2. There may of course be additional uncertainty in the assumption of similar gas-to-dust and carbon-to-hydrogen ratios in the external galaxies as in the Milky Way. However, lowering the abundance of a species does *not* reduce its observed intensity by a similar amount, as is obvious comparing ^{13}CO and CO observations in the Galaxy (Solomon, Scoville, and Sanders 1979). The ^{13}CO abundance is $\sim 1/89$ of the ^{12}C abundance (Wilson, Langer, and Goldsmith 1981), and yet the observed ^{13}CO emission is one-fifth of ^{12}CO emission. Thus even if carbon-to-hydrogen ratios change by an order of magnitude, the H_2 mass derived from *observed* CO emission will change by a much smaller factor.

The only area of disagreement with a constant value of 4×10^{20} for the ratio is in the cloud cores where the mean ratio is a factor of 5 larger. We do not believe such

TABLE 6

CO EMISSION AND H_2 COLUMN DENSITIES FOR MILKY WAY SOURCES

Cloud Sample	No. in Sample	$\langle I_{CO}\rangle$[a] (K km s^{-1})	$\langle I_{CO}/I_{^{13}CO}\rangle$	$\langle N_{H_2}\rangle$[b] (cm^{-2})	$\langle N_{H_2}/I_{CO}\rangle$[c] [cm^{-2} (K km s^{-1})$^{-1}$]
Cloud Core Regions					
Orion KL.....	1	200	5.3	3×10^{23}	1.5×10^{21}
M17SW	1	331	5.9	9×10^{23}	2.7×10^{21}
W30H	1	109	2.4	2×10^{23}	1.8×10^{21}
Dark Nebulae					
Lynds	68	7.9	4.0	1.7×10^{21}	$2.5\pm2\times10^{20}$
Taurus	14	11.7	5.4	5.8×10^{21}	$3.2\pm2\times10^{20}$
Ophiucus	12	23.4	14.4	5.7×10^{21}	$2.5\pm2\times10^{20}$
Giant Molecular Clouds					
$l=24°-30°$ ...	25	59.0	5.7[d]	2.2×10^{22}	$4.2\pm2\times10^{20}$

NOTE.—Data are from Ulich and Haas 1976 for the cloud cores; from Dickman 1978 for the Lynds clouds; from Frerking, Langer, and Wilson 1982 for the Taurus and Ophiucus clouds; and from Solomon, Scoville, and Sanders 1982 for the sample of giant molecular clouds at $l=24°-30°$. The last two samples are likely to be most representative of the regions producing most of the observed emission in the external galaxies since the core regions take up a relatively small area in each cloud, and in the Dickman sample we have included only positions where actual extinction estimates are given (as opposed to limits). Thus, this sample is biased towards clouds of low extinction.

[a]All ^{12}CO integrated intensities were converted to the Kitt Peak scale T_A^* (Ulich and Haas 1976). The radiation temperatures given by Dickman 1978 and the T_A^* at Bell Labs given by Frerking, Langer, and Wilson 1982 were therefore multiplied by factors of 0.65 and 0.85 respectively which are the ratios of the Orion A CO radiation temperature to T_A^* (see Ulich and Haas 1976), and the ratio of T_A^* measured at Bell Labs on Orion to that measured by Ulich and Haas on the NRAO 11 m antenna.

[b]H_2 column densities were derived from visual and IR extinction estimates in the dark clouds (given by Dickman 1978 and Frerking, Langer, and Wilson 1982) and from LTE analysis of ^{13}CO and CO measurements in the cloud cores assuming an abundance ratio $(H_2/^{13}CO)=10^6$ as obtained by Frerking, Langer, and Wilson 1982 in Taurus at $A_v>4$ mag. To convert from extinction to column density we adopt a constant gas-to-dust ratio of $N_{H_2}/A_v=0.94\times10^{21}$ cm^{-2} mag^{-1} (Bohlin *et al.* 1978). The column densities in the giant cloud sample were derived from application of the virial theorem to the measured line widths and sizes (Solomon, Scoville, and Sanders 1982). These virial theorem estimates are within 30% of estimates based on ^{13}CO column densities assuming $N_{H_2}/^{13}CO=10^6$.

[c]Empirical ratio of derived $\langle N_{H_2}/I_{CO}\rangle$ for the sample. The errors given are the 1 σ dispersion of the sample points about the mean.

[d]Only 14 of the 25 clouds were measured in ^{13}CO.

regions are at all representative of the areas producing detectable CO emission in external galaxies (due to their small cross section); they are included here simply for comparison. Adoption of the cloud core ratio for application in the galaxies would *raise* the derived masses by a factor of 5!

As an additional check on our mass estimates, we may make use of the ^{13}CO data obtained on the nucleus of IC 342. For ^{13}CO the column density is given by

$$N_{^{13}CO}=\frac{1.1\times10^{15}\int\tau_{10}\,dv\,\mathrm{cm}^{-2}}{(1-e^{-5.3/T_x})\,f(J=1)}, \qquad \text{(A1)}$$

where T_x is the molecular excitation temperature, τ_{10} is the $J=1$–0 optical depth, and $f(J=1)$ is the fraction of ^{13}CO in $J=1$. *If* the ^{13}CO is optically thin equation (A1) reduces to

$$N_{^{13}CO}=\frac{2.1\times10^{14}I_{^{13}CO}}{f(J=1)\eta_{BEAM}}. \qquad \text{(A2)}$$

Since most of the emission probably arises from low density molecular clouds ($n_{H_2}<10^3$ cm^{-3}), the CO levels will not be highly populated. Non-LTE excitation calculations for this density regime give $f_1=0.26$–0.55 (R. Snell 1981, private communication). Adopting $f(J=1)=0.26$, the observed $I_{^{13}CO}=4$ K km s^{-1} yields $N_{^{13}CO}=5\times10^{15}$ cm^{-2} for assumed optically thin ^{13}CO emission. For an $(H_2/^{13}CO)$ ratio of 10^6 as found by Frerking, Langer, and Wilson (1981) in dark clouds with

$A_v > 5$ mag, we obtain a minimum H_2 column density of 5×10^{21} cm^{-2} for the nucleus of IC 342. A reasonable estimate of the ^{13}CO optical depth is derived from comparison of the observed CO/^{13}CO intensity ratio of 11 in the center of IC 342 with the solar system abundance ratio of (C/^{13}CO) = 89 (i.e., $\tau_{^{13}CO} \approx 8$). It is therefore plausible that when the ^{13}CO column density derived assuming optical thinness is corrected for saturation, the final H_2 column density estimate from ^{13}CO is in reasonable agreement with the estimate of 1.5×10^{22} cm^{-2} derived from ^{12}CO on the basis of our analysis in the first part of this Appendix.

REFERENCES

Ables, H. D. 1971, *Pub. US Naval Obs., Series II*, Vol. 20, Part 4.
Arp, H. C. 1966, *Ap. J. Suppl.*, **14**, 1.
Baker, J. R., Haskam, C. G. T., Jones, B. B., and Wielebinski, R. 1977, *Astr. Ap.*, **59**, 261.
Bania, T. 1980, *Ap. J.*, **242**, 95.
Becklin, E. E., Gatley, I., Mathews, K., Neugebauer, G., Sellgren, K., Werner, M. W., and Wynn-Williams, C. G. 1980, *Ap. J.*, **236**, 441.
Bieging, J. H., Blitz, L., Lada, C. J., and Stark, A. A. 1981, *Ap. J.*, **247**, 443.
Blitz, L., Israel, F. P., Neugebauer, G., Gatley, I., Lee, T. J., and Beattie, D. H. 1981, *Ap. J.*, **249**, 76.
Blitz, L., and Shu, F. H. 1980, *Ap. J.*, **238**, 148.
Bohlin, R. C., Savage, B. D. and Drake, J. F. 1978, *Ap. J.*, **224**, 132.
Boroson, T., 1981, *Ap. J. Suppl.*, **46**, 177.
Burton, W. B., and Gordon M. A. 1978, *Astr. Ap.*, **63**, 7.
Burton, W. B., Gordon, M. A., Bania, T. M., and Lockman, F. J. 1975, *Ap. J.*, **202**, 30.
Cohen, R. S., Cong, H., Dame, T. M., and Thaddeus, P. 1980, *Ap. J. (Letters)*, **239**, L53.
Cohen, R. S., and Thaddeus, P. 1977, *Ap. J. (Letters)*, **217**, L155.
Combes, F., Encrenaz, P. J., Lucas, R., and Weliachew, L. 1977, *Astr. Ap.*, **55**, 311.
_____. 1978, *Astr. Ap. (Letters)*, **67**, L13.
de Vaucouleurs, G. 1979, *Ap. J.*, **227**, 380.
Dickman, R. L. 1978, *Ap. J. Suppl.*, **37**, 407.
Dressel, L. L., and Condon, J. J. 1976, *Ap. J. Suppl.*, **31**, 187.
Eggen, O. J., Lynden-Bell, D., and Sandage, A. 1962, *Ap. J.*, **136**, 748.
Elmegreen, B. G., Elmegreen, D. M., and Morris, M. 1980, *Ap. J.*, **240**, 455.
Encrenaz, P. J., Stark, A. A., Combes, F., and Wilson, R. W. 1979, *Astr. Ap. (Letters)*, **78**, L1.
Freeman, K. C. 1970, *Ap. J.*, **160**, 811.
Frerking, M., Langer, W. D., and Wilson, R. W. 1982, *Ap. J.*, in press.
Gordon, M. A. 1978, *Ap. J.*, **222**, 100.
Huggins, P. J., Gillespie, A. R., Phillips, T. G., Gardner, F. F., and Knowles, S. 1975, *M.N.R.A.S.*, **173**, 69.
Kormendy, J., and Norman, C. A. 1979, *Ap. J.*, **233**, 539.
Morris, M., and Lo, K. Y. 1978, *Ap. J.*, **223**, 803.
Newton, K. 1980*a*, *M.N.R.A.S.*, **191**, 169.
_____. 1980*b*, *M.N.R.A.S.*, **191**, 615.
Penzias, A. A., and Burrus, C. A. 1973, *Ann. Rev. Astr. Ap.*, **11**, 51.
Rickard, L. J., and Palmer, P. 1981, Astr. Ap., in press.
Rickard, L. J. 1979, in *IAU Symposium 84, The Large Scale Characteristics of the Galaxy*, ed. W. B. Burton (Dordrecht: Reidel), p. 413.
Rickard, L. J., and Palmer, P. 1981, *Astr. Ap.*, in press.
Rickard, L. J., Palmer, P., Morris, M., Turner, B. E., and Zuckerman, B. 1977, *Ap. J.*, **213**, 673.
Rickard, L. J., Palmer, P., Morris, M., Zuckerman, B., and Turner, B. E. 1975, *Ap. J. (Letters)*, **199**, L75.
Rickard, L. J., Turner, B. E., and Palmer, P. 1977, *Ap. J. (Letters)*, **218**, L51.
Rieke, G. H., and Lebofsky, M. J. 1978, *Ap. J. (Letters)*, **220**, L37.
Rogstad, D. H., and Shostak, G. S. 1972, *Ap. J.*, **176**, 315.
Rogstad, D. H., Shostak, G. S., and Rots, A. H. 1973, *Astr. Ap.*, **22**, 111.
Rowan-Robinson, M., Phillips, T. G., and White, G. 1980, *Astr. Ap.*, **82**, 381.
Rubin, V. C., Ford, W. K., and Thonnard, N. 1980, *Ap. J.*, **238**, 471.
Sandage, A., and Tammann, G. 1974, *Ap. J.*, **194**, 559.
Sanders, R. H. 1979, in *IAU Symposium 84, The Large Scale Characteristics of the Galaxy*, ed. W. B. Burton (Dordrecht: Reidel), p. 383.
Sanders, D. B., Solomon, P. M., and Scoville, N. Z. 1981, in preparation.
Schweizer, F. 1976, *Ap. J. Suppl.*, **31**, 313.
Scoville, N. Z., and Solomon, P. M. 1975, *Ap. J. (Letters)*, **199**, L105.
Scoville, N. Z., and Solomon, P. M., and Jefferts, K. B. 1974, *Ap. J. (Letters)*, **187**, L63.
Scoville, N. Z., and Young, J. S. 1982, in preparation.
Searle, L., Sargent, W. L. W., and Bagnuolo, W. G. 1973, *Ap. J.*, **179**, 427.
Seiden, P. E., and Gerola, H. 1979, *Ap. J.*, **233**, 56.
Smith, M. G., and Weedman, D. W. 1970, *Ap. J.*, **161**, 33.
_____. 1971, *Ap. J.*, **169**, 271.
Solomon, P. M., and de Zafra, R. 1975, *Ap. J. (Letters)*, **199**, L79.
Solomon, P. M., Sanders, D. B., and Scoville, N. Z. 1979, in *IAU Symposium 84, The Large Scale Characteristics of the Galaxy*, ed. W. B. Burton (Dordrecht: Reidel), p. 35.
Solomon, P. M., Scoville, N. Z., and Sanders, D. B. 1979, *Ap. J. (Letters)*, **232**, L89.
_____. 1982, in preparation.
Stark, A. A. 1979, Ph.D. thesis, Princeton University.
Telesco, C. M., and Harper, D. A. 1980, *Ap. J.*, **235**, 392.
Tully, R. B. 1974, Ph.D. thesis, University of Maryland.
Ulich, B. L., and Haas, R. W. 1976, *Ap. J. Suppl.*, **30**, 247.
van der Kruit, P. C. 1973, *Astr. Ap.*, **29**, 249.
van der Kruit, P. C., Allen, R. J., and Rots, A. H. 1977, *Astr. Ap.*, **55**, 421.
Wilson, R. W., Langer, W. D. and Goldsmith, P. F. 1981, *Ap. J. (Letters)*, **243**, L47.
Young, J. S., Scoville, N. Z., and Tacconi, L. 1982, in preparation.

Note added in proof.—We have recently discovered molecular rings in two Sb galaxies, NGC 7331 and NGC 2841 (Young and Scoville 1982, *Ap. J.* [*Letters*], submitted). These new observations permit us to discriminate between the nuclear bulge and ILR hypotheses of ring origin (see § IV*c*), inasmuch as the peaks in the optical and H I rotation curves coincide in radius with the peaks in the CO radial distributions. Since the ILR should occur *outside* of the rotation curve peak, these new data favor the nuclear bulge hypothesis for the origin of molecular rings.

NICK Z. SCOVILLE and JUDITH S. YOUNG: Five College Radio Astronomy Observatory, University of Massachusetts, Amherst, MA 01003